ELSEVIER

Journal of Fluids and Structures 20 (2005) 425–449

JOURNAL OF FLUIDS AND STRUCTURES

www.elsevier.com/locate/jfs

Investigation of Strouhal frequencies of two staggered bluff bodies and detection of multistable flow by wavelets

Md. Mahbub Alam[a,*], H. Sakamoto[b]

[a]*Department of Mechanical Engineering, The Hong Kong Polytechnic University, Hung Hom, Kowloon, Hong Kong*
[b]*Department of Mechanical Engineering, Kitami Institute of Technology, 165 Koen-cho, Kitami, Hokkaido 090-8507, Japan*

Received 25 November 2003; accepted 10 November 2004

Abstract

The results of a wind tunnel investigation of the Strouhal frequencies of two identical, stationary, parallel circular cylinders arranged in staggered configurations, carried out in a uniform cross-flow at a Reynolds number of 5.5×10^4, are presented in this paper. Results of measurements of the Strouhal frequencies of a square cylinder (prism) and a circular cylinder arranged in tandem and in some selected staggered configurations are also presented. In the case of two circular cylinders, the investigation was performed at staggered angles of $\alpha = 10^\circ$, 25°, 45°, 60° and 75° in the range of $T/D = 0.1-5.0$, where α is the angle between the free-stream flow and the line connecting the centers of the cylinders, T is the gap width between the cylinders, and D is the diameter of a cylinder. The new findings in this study for two circular cylinders are: (i) three stable flow patterns with regard to Strouhal numbers were identified for $\alpha = 25^\circ$ in the range of $T/D = 1.1-1.8$ and (ii) two stable flow patterns with regard to Strouhal numbers were identified for $\alpha = 45^\circ$ in the range of $T/D = 0.8-2.1$. Intermittent mutual lock-in of the two frequencies of two cylinders caused such multistable flow patterns. These multistable flow patterns and the intermittent lock-in phenomenon were elucidated from wavelet analysis results of fluctuating pressures simultaneously stored from the surfaces of the cylinders. Strouhal number distributions for $\alpha = 60^\circ$ and 75° were almost the same in nature as those of $\alpha = 45^\circ$. When a square cylinder and a circular cylinder were arranged at $\alpha = 25^\circ$ with the square cylinder being used as the upstream cylinder, the downstream cylinder was found to shed vortices always in synchronization with the upstream cylinder. For $\alpha = 60^\circ$, when the square cylinder was used as the upstream cylinder, both cylinders were found to be locked-in to shed vortices with an intermediate Strouhal number for a certain range of values of T/D.

1. Introduction

In many engineering applications of cylinder-like structures, i.e., groups of chimney stacks, tubes in heat exchangers, overhead power-line bundles, bridge piers, stays, masts, chemical reaction towers, off-shore platforms, adjacent skyscrapers, etc., fluid forces, Strouhal frequencies and flow configurations are major criteria for the design of structures. The vortex-shedding frequency often characterizes the flow field around structures and is an important factor in estimation of the response of a structure or groups of structures immersed in a cross-flow. The present study, a detailed investigation of Strouhal frequencies and wake interactions of two staggered circular cylinders and of a circular

*Corresponding author. Tel.: +852 2766 7813; (office), 852 6573 3951(mob); fax: +852 2365 4703.
E-mail addresses: mmalam@polyu.edu.hk, alamm28@yahoo.com (M.M. Alam).

0889-9746/$ - see front matter © 2005 Elsevier Ltd. All rights reserved.
doi:10.1016/j.jfluidstructs.2004.11.003

cylinder and a square cylinder in some selected configurations, was motivated by both fundamental and practical considerations.

1.1. Review of previous works

Though the staggered arrangement is perhaps the configuration most commonly found in engineering applications, numerous investigations on the flows past two circular cylinders in side-by-side and tandem arrangements have been performed, but investigations pertaining to two staggered cylinders are relatively few, particularly investigation of the vortex-shedding processes in terms of the Strouhal frequencies of two staggered cylinders. Zdravkovich (1977) and Chen (1986) reviewed a number of papers pertaining to flow interactions of two cylinders in various arrangements.

Flow interaction and fluid forces acting on two staggered cylinders have been investigated by Hori (1959), Price (1976), Zdravkovich and Pridden (1977), Zdravkovich (1980), Bokaian and Geoola (1984), Price and Paidoussis (1984), Ko and Wong (1992) and Gu et al. (1993). With regards to the vortex-shedding frequency and formation of the wake behind two staggered cylinders, the features of flow over and behind the staggered cylinders are foreseen to be very complex. Extensive measurements of vortex-shedding frequencies were performed by Kiya et al. (1980); however, they failed to detect a vortex-shedding frequency behind the upstream cylinder in some cases. Further measurements of vortex-shedding frequencies have been performed by Ishigai et al. (1972), Bokaian and Geoola (1984), Ko and Wong (1992), Sun et al. (1992), Gu and Sun (1999), and Sumner et al. (2000). However, their measurements were restricted to only a narrow range of staggered arrangement, indicating that further investigations are necessary to obtain insight into the vortex-shedding processes of two staggered cylinders.

As has been revealed in the previous studies, for a small value of T/D (see Fig. 1 for definitions of symbols), i.e., when the downstream cylinder is fully or partially submerged into the upstream cylinder wake, the two cylinders behave like a single body and the frequencies of vortex shedding behind the two cylinders are the same. For an intermediate value of T/D, at which narrower and wider wakes are formed behind the upstream and downstream cylinders, respectively, the frequencies of vortex shedding behind the upstream and downstream cylinders are of a higher and lower magnitude, respectively. For a higher value of T/D, i.e., when each cylinder sheds vortices independently, the frequency of vortex shedding behind each cylinder is the same as that in the case of a single, isolated cylinder. The vortex-shedding processes from the cylinders for an intermediate value of T/D are very complex in relation to defining frequencies and shedding processes of the individual shear layers (Fig. 1) of the upstream and downstream cylinders. Sumner et al. (2000) tried to determine the vortex-shedding frequency of the individual shear layers by counting vortices shed from them in flow visualization tests. However, their approach failed to differentiate frequencies of a shear layer if the shear layer sheds vortices at more than one frequency. For an intermediate value of T/D, they found that the two frequencies, due to the formation of a narrower and wider wake behind the upstream and downstream cylinders, respectively, are associated with the individual free shear layers, rather than with the individual cylinders; i.e., the inner and outer free shear layers of the downstream cylinder shed vortices at different frequencies, the outer shear layer shedding vortices at a lower frequency, and the inner shear layer shedding vortices at a higher frequency equal to that of the shear layers of the upstream cylinder.

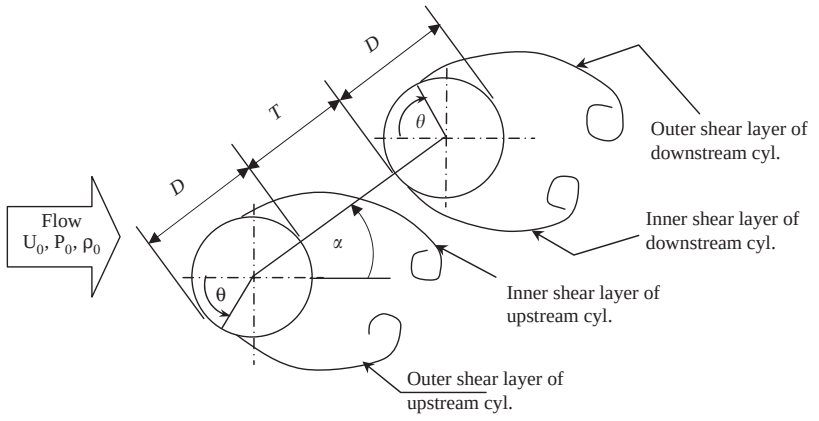

Fig. 1. Notation for staggered configuration.

When this paper was close to completion, a report was published by Sumner and Richards (2003) showing some intriguing data resembling the results of the present study. It is known that, for two staggered circular cylinders with an intermediate value of T/D, the narrower wake behind the upstream cylinder corresponds to a higher frequency and the wider wake behind the downstream cylinder corresponds to a lower frequency. For such an intermediate value of T/D, i.e., for $T/D = 1.0$ ($\alpha = 16-75^\circ$), power spectrum data of fluctuating velocity obtained by Sumner and Richards (2003) show that both the higher and lower Strouhal numbers exist in the upstream wake. For the same value of $T/D = 1.0$ ($\alpha = 16-55^\circ$), both the higher and lower Strouhal numbers also exist in the downstream wake. These findings imply that there is a special nature of flow patterns that causes the two different Strouhal numbers in a wake. However, Sumner and Richards did not discuss the significance of the appearance of two Strouhal numbers in each of the upstream and downstream wakes. A clear discussion on the presence of two different Strouhal numbers in the wake is presented in this paper.

In the previous investigations, vortex-shedding frequencies were measured from fluctuating velocities in the wakes. However, vortex-shedding frequency measured from velocity fluctuation is strongly dependent on the measurement location in the wake (Spivack, 1946; Ishigai et al., 1972; Kiya et al., 1980; Cimbala and Krein, 1990; Sumner et al., 2000), and it may sometimes differ from the frequency of fluctuating lift force or fluctuating surface pressure, especially in the case of multiple cylinders. The appropriate location of the hot-wire to be placed in a wake to measure the frequency of individual shear layers is very difficult to determine, especially when two cylinders are placed at an intermediate value of T/D, because phenomena like gap vortex pairing, enveloping of the gap vortex pair and splitting of the gap vortex pair are found to occur for an intermediate value of T/D (Sumner et al., 2000). On the other hand, if a switching of flow occurs, there is more than one trajectory and more than one rolling position of a shear layer in a wake, and sufficient information on the characteristics of the shear layer cannot be obtained by placement of a hot-wire at one location in the wake for such a case. Also, energy levels at different frequencies of vortices shed from the cylinders, if there are two or more frequencies in a wake, are difficult to be differentiated because energy level is also dependent on the measurement location in the wake (Kiya et al., 1980; Guillaume and LaRue, 1999; Konstantinidis et al., 2002). To estimate the response of a structure as well as to design a structure, indeed, the frequency of fluctuating pressure acting on the structure is more reliable than the frequency associated with wake velocity. Considering the above points, the frequency was estimated from the fluctuating surface pressure acting on the cylinders in the present study.

1.2. Scope of the study

The compilation of the previous investigations on two staggered cylinders in the previous section indicates that the vortex-shedding frequency and the behavior of the individual shear layers are not yet clear, despite the fact that the behavior of the individual shear layers plays an important role in the interaction between the wakes of the two staggered cylinders. The objectives of this study were (i) to measure the vortex-shedding frequencies of the individual shear layers, (ii) to elucidate wake interactions with regard to vortex-shedding frequency, and (iii) to detect multistable flow by using wavelet analysis. The present paper presents a series of vortex-shedding frequency measurement results and a mutual discussion on vortex-shedding frequencies, flow patterns, and interactions between the upstream and downstream wakes of two staggered circular cylinders. Strouhal frequencies were estimated from Fourier power spectra of fluctuating surface pressures on both sides of each cylinder for $\alpha = 10^\circ$, 25°, 45°, 60°, and 75°. Results of measurements of the Strouhal frequencies of a square cylinder and a circular cylinder arranged in tandem and in staggered configurations with $\alpha = 25^\circ$ and 60° are also presented in this paper. The behavior of the individual shear layers and the appearance of multistable flow identified by wavelet analysis are discussed.

1.3. Wavelet analysis

The Fourier transform provides averaged spectral coefficients that are independent of time, i.e., spectral coefficients are fully localized in the frequency domain and infinitely distributed in the time domain when Fourier transforms are employed in a signal. It is useful for a stationary signal, of which frequency and amplitude do not change with time. However, many processes we face in practical cases are essentially nonstationary, in which amplitude and/or frequency change with time, such as the sound pressure recorded from speech and music, vibration of a structure due to fluctuating wind loads, and velocity or pressure signals specially in a wake of multiple cylinders. If the Fourier transform is employed in a nonstationary signal, information on frequency and intensity of energy with change in time is impossible to be traced out. A scan analysis using the so-called short-term Fourier transform (STFT) is used in this case. However, it also has some limitations as described by Daubechies (1990), Newland (1993), Hamdan et al. (1996), and Torrence and Compo (1998). The limitations of STFT are mostly overcome by using the wavelet transform which

produces a potentially more revealing picture of the time–frequency localization of signals. However, wavelet analysis is relatively new and it has not yet been applied to its full potential in the areas of fluid mechanics. Li (1997, 1998) and Yilmaz and Kodal (2000) used wavelet analysis to identify dominant frequencies in a coaxial jet flow, and Hamdan et al. (1996) used it in self-excited flow-induced vibration. Recently, Alam et al. (2003a, b) used wavelet and cross-wavelet transforms to trace out characteristics of switching flow which occurs for certain configurations of two circular cylinders in tandem and side-by-side arrangements. For wavelet maps of two simultaneously obtained hot-wire signals in the wakes of two side-by-side cylinders at a bistable flow spacing, Alam et al. (2003a) interestingly showed, how the wake frequency of a cylinder changes with respect to that of the other and with respect to time. They also used cross-wavelet analysis to trace out the synchronized frequency, the synchronized region in time–space, and phase characteristics between two signals of two cylinders. The wavelet transform is a linear convolution (Yong, 1998) of a given one-dimensional signal $p(t)$ which is to be analyzed and the mother wavelet $\psi(t)$. Mathematically, the wavelet transform is written as

$$W(s,b) = \frac{1}{\sqrt{s}} \int p(t)\psi^*\left(\frac{t-b}{s}\right) \mathrm{d}t, \tag{1}$$

where $W(s, b)$ is the wavelet coefficient, the superscripted asterisk denotes the complex conjugate, b is the translation parameter, and s is the scale parameter.

Though there are many mother wavelets used in practice, the Mexican hat wavelet, Gabor wavelet and Morlet wavelet are commonly used in the field of fluid mechanics (Hamdan et al., 1996; Li, 1997; Li and Nozaki, 1997; Kareem and Kijewski, 2002). The wavelet map is a graphical representation of $W(s, b)$ of two variables s and b for a given mother wavelet. A large value of $W(s, b)$ reflects the combined effect of a large fluctuation of the signal and of good matching of shape between the signal and the wavelet. The Mexican hat wavelet is real-valued, and the Morlet and Gabor wavelets are complex-valued. The real-valued wavelet isolates local minima and maxima of a signal. When a complex-valued mother wavelet is used in Eq. (1), $W(s, b)$ becomes complex; hence $W(s, b)$ has a real part and an imaginary part, $W_R(s, b)$ and $W_I(s, b)$, respectively. When only the instantaneous frequency of a signal is important to be identified, the values of $W^2(s,b) = W_R^2(s,b) + W_I^2(s,b)$ are plotted against the frequency and time scales (Farge, 1992). However, when the minima and maxima of a signal are important to be identified with regard to frequency, only the values of $W_R(s, b)$ can be plotted against the frequency and time scales.

The choice of appropriate mother wavelet, however, depends on the kind of information that we want to extract from the signal. For example, information obtained by using the Mexican hat wavelet is highly localized in time–space and poorly localized in frequency space. The Gabor wavelet has somewhat better frequency resolution properties and a poorer time resolution properties than the Mexican hat. On the other hand, the Morlet wavelet has somewhat better frequency resolution and somewhat poorer time resolution properties than the Gabor wavelet. In this work, both the Morlet and Gabor wavelets are used depending on the situations and on the characteristics of the signal.

The Morlet wavelet is expressed as

$$\psi(t) = \pi^{-1/4} \mathrm{e}^{i\omega_0 t} \mathrm{e}^{-t^2/2} \tag{2}$$

and the Gabor wavelet is expressed as

$$\psi(t) = \left(\frac{\omega_0}{\gamma}\right)^{1/2} \pi^{-1/4} \mathrm{e}^{i\omega_0 t} \mathrm{e}^{-(\omega_0 t/\gamma)^2/2}, \tag{3}$$

where $\gamma = \pi\sqrt{2/\ln 2}$ and ω_0 is the number of wave in the wavelets. In practice, if we take $\omega_0 = 6.0$, the wavelets are marginally admissible (Farge, 1992; Li, 1997). However, a higher value of ω_0, such as $\omega_0 = 12$, can be chosen when the frequency resolution of a signal is more important than the time resolution (Alam et al., 2003b).

2. Experimental details

The experiments were conducted in a closed-circuit wind tunnel having a test-section of 0.3 m in width, 1.2 m in height and 2.2 m long. The cylinders used as test models were made of brass and were each 49 mm in diameter. The cylinders spanned the horizontal 0.3 m dimension of the tunnel. The free-stream velocity, U_0, in the tunnel was 17 m s^{-1}, giving a Reynolds number (Re) of 5.5×10^4, based on the free-stream velocity and the diameter of a cylinder. Within the middle 0.24 m × 0.95 m of the test-section, the flow was uniform within $\pm 2\%$ of the centerline velocity. Within the same region, the longitudinal turbulence intensity, when the tunnel was empty, was less than 0.5%. In order to check the spanwise uniformity of flow as well as spanwise separation of flow over a single circular cylinder, circumferential

time-averaged and fluctuating pressures on the surface of the cylinder at the mid-section, and at ± 35 and ± 80 mm (from the mid-section), were measured. The results showed that the time-averaged and fluctuating pressure distributions at the five different sections were the same within the accuracy of measurement. The geometric blockage and the aspect ratios per cylinder at the test-section were 4% and 6, respectively.

Fig. 1 is a schematic diagram showing an arrangement of two cylinders, definitions of symbols and coordinate systems. The stagger angle α is defined as the angle between the free-stream flow and the line connecting the centers of the two cylinders. T is the gap width between the cylinders, as opposed to center-to-center spacing adopted by other researchers. The position of any point on the surface of a cylinder is denoted by θ measured from the free-stream direction; the value of θ is considered as positive (0–180°) for the outer surfaces and negative (0–−180°) for the inner surfaces of the cylinders. Vortex-shedding frequencies were measured from fluctuating surface pressures at $\theta = \pm 90°$ on each of the two cylinders. It is supposed that the pressure signals at $\theta = 90°$ and $-90°$ capture information on the characteristics of the outer and inner shear layers, respectively. It is noted that the Strouhal number estimated from the pressure signal received from the surface of a cylinder does not depend on the peripheral position ($\theta = 10-170°$) of the pressure tap, except in the base region ($\theta = 170-190°$). In other words, if the pressure tap is located at a different position (except in the base region) from the separation position of a shear layer, the Strouhal number estimated from the pressure signal received at that position will be the same as that received at the separation position of the shear layer (Alam et al., 2003c). Pressure signals were digitized with a sampling frequency of 3.6 kHz corresponding to about 20 and 120 samples/period for maximum and minimum frequencies detected during experiment. Fourier power spectra of the pressure signal were based on the average of five runs, each run composed of 1024 samples.

A semiconductor pressure transducer (Toyoda PD104 K) located at the mid-section of each cylinder was used to measure the surface pressure during the experiments, and the transducer output was calibrated to give a reading of 6.22 V for 1 kPa of applied pressure. The pressure transducer was set just below the surface of each cylinder and communicated to the surface through a pressure connection of size 0.8 mm diameter by 1.5 mm long, as shown in Fig. 2. The dynamic response characteristics of the transducer were in the range of frequency 0–550 Hz. The transducer responded reasonably to the pressure fluctuations up to 500 Hz with a gain factor of 1 ± 0.06, the phase lag being negligible. This frequency was well above the frequency detected in the present experiments. The experiments were performed for $\alpha = 0°$, 10°, 25°, 45°, 60° and 75° in the range of $T/D = 0.1-5.0$. The settings of T/D were 0.1, 0.2, 0.3, 0.5, 0.6, 0.7, 0.8, 0.9, 1.1, 1.2, 1.5, 1.8, 2.1, 2.4, 2.7, 3.0, 3.5, 4.0, 4.5 and 5.0. The uncertainties in spacing ratio T/D and staggered angle α were estimated to be ± 0.005 and $\pm 0.3°$, respectively. The overall uncertainty in the measurements of

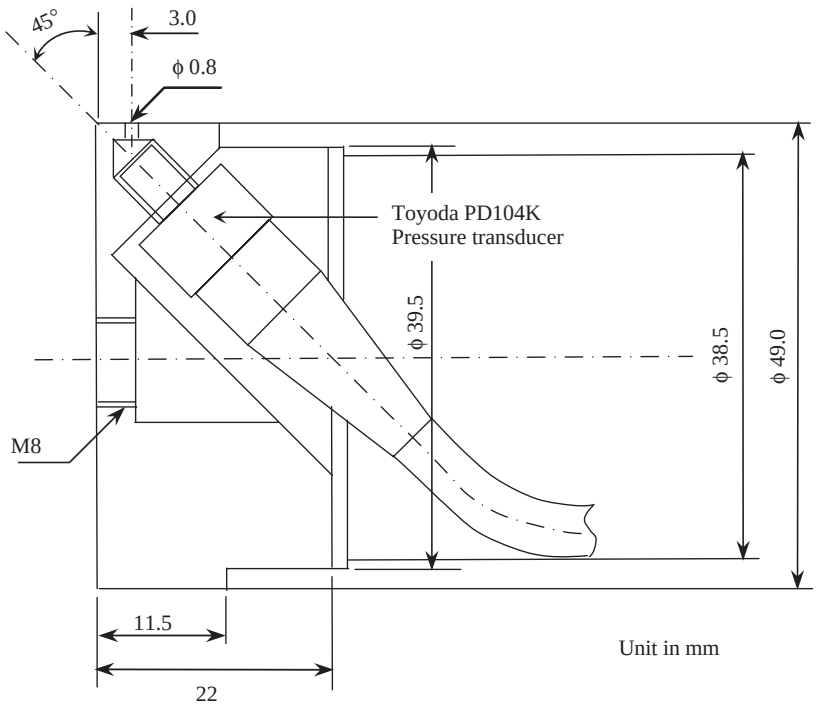

Fig. 2. Installation of a pressure transducer inside a cylinder.

Strouhal numbers was estimated to be 2%. The Strouhal numbers presented in this study were not corrected for the effects of wind-tunnel blockage or aspect ratio; this is because of complexity of doing so when there is flow interference between two cylinders.

3. Results and discussion

3.1. Tandem and side-by-side arrangements, $\alpha = 0^\circ$ and 90°

The well-known critical geometry of two cylinders is the tandem and side-by-side arrangements. The tandem arrangement is the critical geometry between staggered configurations of $\alpha = 0^\circ+$ and $\alpha = 0^\circ-$. For $\alpha = 0^\circ+$ (say 5°), only the upper shear layer of the upstream cylinder reattaches onto the upper surface of the downstream cylinder; for $\alpha = 0^\circ-$ (say $\alpha = -5^\circ$), only the lower shear layer of the upstream cylinder reattaches onto the lower surface the downstream cylinder, as labelled in Fig. 1. Hence, for $\alpha = 0^\circ$, the upper and lower shear layers of the upstream cylinder reattach alternately onto the upper and lower surfaces of the downstream cylinder, respectively, specially for $T/D < 2.0$ (Igarashi, 1981, 1984; Sumner et al., 2000; Alam et al., 2003c). On the other hand, the side-by-side arrangement is the critical geometry between staggered configurations of $\alpha = 90^\circ-$ and $\alpha = 90^\circ+$. For $\alpha = 90^\circ-$ (say $\alpha = 85^\circ$), the gap flow is biased toward the lower cylinder (Fig. 1); for $\alpha = 90^\circ+$ (say $\alpha = 95^\circ$), the gap flow is biased toward the upper cylinder. Hence, for $\alpha = 90^\circ$, the gap flow switches intermittently to be biased toward each of the cylinders. Recently Alam et al. (2003a, b, c) measured the Strouhal frequency from the fluctuating lift and fluctuating pressure for two circular cylinders in side-by-side and tandem arrangements. In the case of two side-by-side cylinders, Alam et al. (2003a) found three modes of flow corresponding to three modes of Strouhal numbers for $T/D < 1.2$. Two of the three modes were previously known: narrower and wider wake modes, due to biased gap flow, corresponding to a higher and lower Strouhal numbers, respectively (Spivack, 1946; Bearman and Wadcock, 1973; Kamemoto, 1976; Kiya et al., 1980). The other mode was the nonbiased flow pattern corresponding to a Strouhal number equal to that of a single, isolated cylinder. Actually, the nonbiased flow pattern found by Alam et al. (2003a) can be attributed for $\alpha = 90^\circ$ and the other two are contributed from $\alpha = 90^\circ-$ and $\alpha = 90^\circ+$.

In the case of two tandem cylinders, the Strouhal frequency of the downstream cylinder synchronizes with that of the upstream cylinder. In other words, the Strouhal frequency of the downstream cylinder is always triggered by the alternating shear layers of the upstream cylinder (for $T/D < 3$) or by the incident vortices from the upstream cylinder (for $T/D > 3$) (Ishigai, 1972; Igarashi, 1981; Alam et al., 2002a, b, 2003c). In order to check whether the synchronization of the downstream cylinder Strouhal frequency to the frequency of incident vortices from the upstream cylinder is a unique property of the flow, reduction and increase of the vortex-shedding frequency of the upstream cylinder with respect to the single cylinder vortex-shedding frequency of the downstream cylinder were done by (i) a replacement of the upstream cylinder by a square cylinder, i.e., a square cylinder and a circular cylinder in tandem arrangement and (ii) a replacement of the downstream cylinder by a square cylinder, i.e., a circular cylinder and a square cylinder in tandem arrangement, as shown in Fig. 3. Note that the cross-section of the square cylinder was 42 mm × 42 mm and the diameter of the circular cylinder was 49 mm. Strouhal numbers for the square and circular cylinders, when they were used as a single, isolated cylinder, were 0.125 (50 Hz) and 0.18 (64 Hz), respectively. These values of Strouhal numbers are somewhat smaller than those $St = 0.13$ (square cylinder, $Re = 3.3 \times 10^4$) measured by Lesage and Gartshore (1987), $St = 0.13$ (square cylinder, $Re = 3 \times 10^3$) measured by Nakagawa et al. (1999), $St = 0.195$ (circular cylinder, $Re = 6.5 \times 10^4$) measured by Lesage and Gartshore (1987), $St = 0.19$ (circular cylinder, $Re = 1.58 \times 10^4$) measured by Kiya et al. (1980), and $St = 0.2$ (circular cylinder, $Re = 4.4 \times 10^4$) measured by Schewe (1983). This is because of a low aspect ratio prevailing in the present study (Zdravkovich, 1981).

The results for the two cases mentioned above are shown in Fig. 3. The vortex-shedding frequencies were obtained from power spectra of the fluctuating pressures on the side surfaces of the cylinders and were nondimensionalized to Strouhal numbers based on the dimension of the upstream cylinder. For both the cases, the spacing between the cylinders was nondimensionalized by dividing by the diameter of the circular cylinder. The figure shows that, for both cases, the downstream cylinder sheds vortices at the frequency of the alternating shear layers of the upstream cylinder (for spacing less than critical one) or at the frequency of the incident vortices from the upstream cylinder (for spacing beyond the critical one). That is, the downstream cylinder is forced to shed vortices in synchronization with the vortex-shedding frequency of the upstream cylinder. Thus, the synchronization of vortex-shedding of the downstream cylinder with that of the upstream cylinder is unique for the tandem configuration. In other words, the vortex-shedding frequency of the downstream body is not so dependent on the cross-sectional shape of the downstream or upstream body; rather it mainly depends on the shedding frequency and strength of vortices that are shed from the upstream

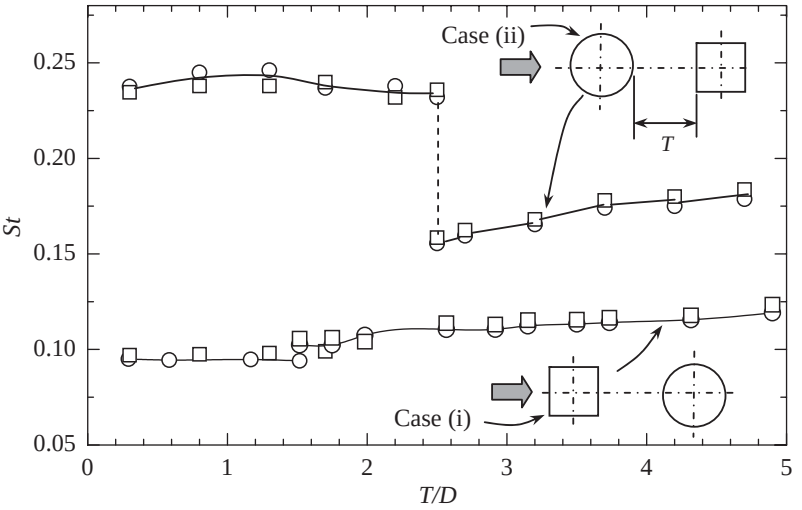

Fig. 3. Strouhal number distributions for a square cylinder and a circular cylinder in tandem arrangement: ○, circular cylinder; □, square cylinder. The Strouhal number was calculated based on the upstream cylinder diameter or width.

body. Such synchronization can be expressed as a tandem effect. Investigations on two tandem cylinders in which a placement of control object on the upstream cylinder significantly increases the Strouhal number of the upstream cylinder also support such synchronization (Alam et al., 2002a, b). It can also be mentioned that two tandem cylinders subjected to forced excitation are induced to be locked-in for a much wider range of excitation frequency than an isolated, single cylinder (Mahir and Rockwell, 1996). It is seen in the figure that, for spacing less than the critical one, Strouhal numbers for the cases (i) and (ii) are smaller and greater than that of the single cylinder value, respectively, implying the shear layers separating from the square cylinder reattach onto the downstream cylinder for the case (i) and the shear layers separating from the upstream circular cylinder pass over the square cylinder without any reattachment onto the downstream cylinder for the case (ii) (Igarashi, 1984). For spacing less than the critical one, in the first case, the shear layers separating from the upstream cylinder reattach onto the downstream cylinder in alternating fashion and alternating vortices are shed only from the downstream cylinder. Now a question may arise: can the Strouhal number be attributed to the downstream cylinder only? Actually, there is a significant contribution of the upstream cylinder in the vortex formation behind the downstream cylinder. As the shear layers of the upstream cylinder shed in alternating fashion at the same frequency of the vortex shedding behind the downstream cylinder, the Strouhal number can be attributed to the upstream cylinder also. On the other hand in the second case, the shear layers separating from the upstream circular cylinder pass over the square cylinder without any reattachment onto the downstream cylinder, and alternating vortices are shed behind the downstream cylinder. Here the upstream cylinder sheds vortices behind the downstream cylinder. Now the question is, which cylinder is the owner of the Strouhal number?

3.2. Two circular cylinders in staggered arrangement

3.2.1. Staggered arrangement with $\alpha = 10^\circ$

Fig. 4(a) shows Strouhal number distributions of two staggered circular cylinders for $\alpha = 10^\circ$ with change in T/D. Here, the Strouhal numbers were measured from fluctuating surface pressure at $\theta = \pm 90^\circ$ for each of the cylinders. The flow pattern for $T/D < 2.1$ is that the inner shear layer separating from the upstream cylinder reattaches onto the outer surface of the downstream cylinder and no Karman vortex forms immediately behind the upstream cylinder. However, for $T/D > 2.4$, fully developed Karman vortices are generated from the upstream cylinder. The figure shows two sets of Strouhal number values for $T/D < 1.3$. The values of Strouhal number for the upper set are somewhat scattered around $St = 0.47$ and the values for the lower set are approximately 0.09. A typical Fourier power spectrum of fluctuating pressure on the downstream cylinder at $\theta = 90^\circ$ (outer side surface), showing two dominant peaks, is presented in Fig. 4(b). The two peaks are due to a bistable nature of two flow patterns. The bistable flow was clearly detected from pressure signals of the downstream cylinder for $T/D < 1.3$. A pressure signal at $\theta = -40^\circ$, where the pressure difference for the two modes was maximum, is shown in Fig. 4(d). A simple sketch of the two flow patterns (modes 1 and 2), which are responsible for such a bistable flow, is shown in Fig. 5. The figure was sketched in light of data obtained in the

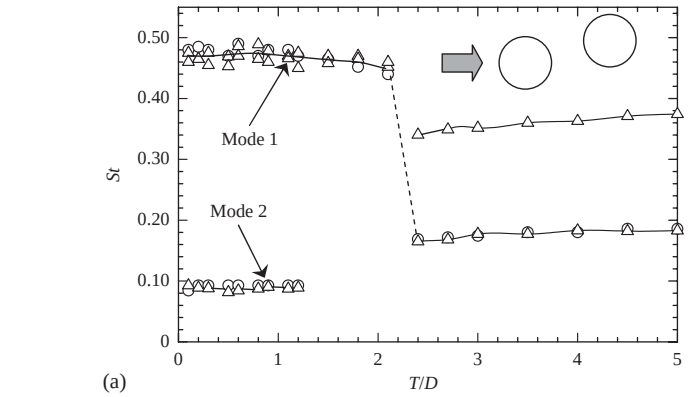

(a)

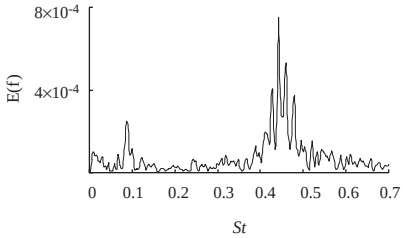

(b) Downstream cylinder, $T/D = 1.0$ ($\theta = 90°$).

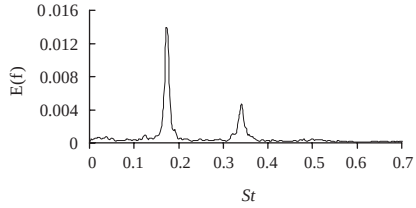

(c) Downstream cylinder, $T/D = 3.0$ ($\theta = -90°$).

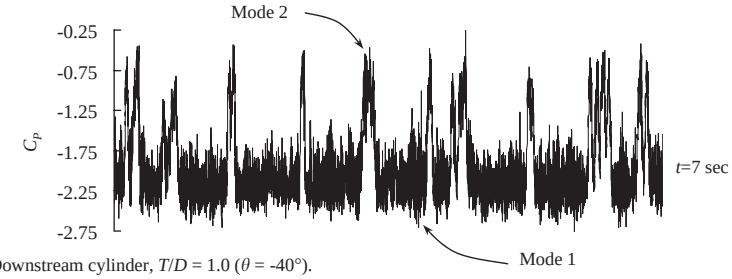

(d) Downstream cylinder, $T/D = 1.0$ ($\theta = -40°$).

Fig. 4. (a) Strouhal number distributions for $\alpha = 10°$: ○, upstream cylinder; △, downstream cylinder; (b), (c) power spectra of fluctuating pressures of the downstream cylinder; (d) pressure signal showing bistable nature of modes 1 and 2.

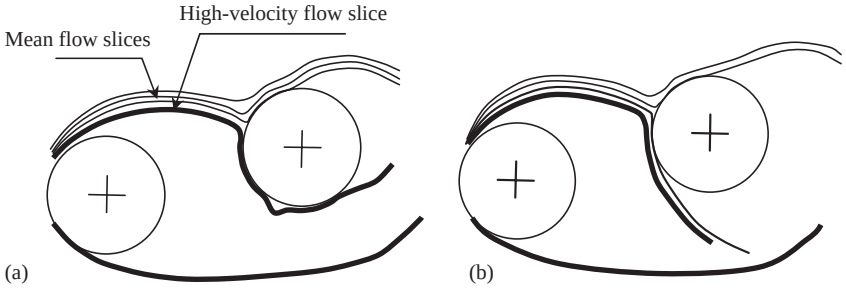

Fig. 5. Sketch of flow patterns for $T/D < 1.3$: (a) mode 1, (b) mode 2.

present study and of the discussion presented in the previous articles [see Zdravkovich (1977), Gu and Sun (1999), Sumner et al. (2000)]. In mode 1, the high-speed part of the reattached shear layer sweeps along the inner surface of the downstream cylinder for a longer peripheral length. In mode 2, the high-speed part together with a share of mean flow separates from the inner surface of the downstream cylinder. Such kind of bistable flow was also detected by Gu and

Sun (1999). Based on time-averaged and fluctuating pressure distributions, as we investigated the two flow patterns of the bistable flow, modes 1 and 2 were consistent with Patterns II_B and III_B, respectively, defined by Gu and Sun (1999). Further details on the flow patterns, modes 1 and 2, can be found in Gu and Sun (1999). Mode 1 corresponds to the higher set of the Strouhal numbers for both the cylinders and mode 2 corresponds to the lower set of the Strouhal numbers for both the cylinders. In other words, in mode 1, Strouhal numbers measured at $\theta = \pm 90^\circ$ of the upstream cylinder and at $\theta = \pm 90^\circ$ of the downstream cylinder were the same and equal to the higher one (≈ 0.47). Similarly, in mode 2, Strouhal numbers measured at $\theta = \pm 90^\circ$ of both the cylinders were the same and equal to the lower one (≈ 0.09). Gu and Sun (1999) also found such higher Strouhal numbers for Pattern II_B (mode 1), but they did not find a definite Strouhal number for Pattern III_B (mode 2). This can be attributed to the location of their measuring probe. Thus $\alpha = 10^\circ$ is a critical staggered angle for modes 1 and 2 for the range of $T/D = 0.1-1.3$. Actually, the critical staggered angle is not a specific angle; rather it has a range in which modes 1 and 2 appear intermittently. However, the actual range of critical staggered angle depends on T/D, as found by Gu and Sun (1999). At $\alpha = 10^\circ$, mode 1 is contributed from $\alpha < 10^\circ$ (roughly from $\alpha = 5-9^\circ$) and mode 2 is contributed from $\alpha > 10^\circ$ (Gu and Sun, 1999). In other words, only one flow pattern resembling mode 1, flow with a higher Strouhal number on both the cylinders, can be found for $\alpha = 5-9^\circ$ and only one flow pattern resembling mode 2, flow with a lower Strouhal number on both the cylinders, can be found for $\alpha > 10^\circ$. For example, a lower Strouhal number on both of the cylinders is found for $\alpha = 25^\circ$ with $T/D = 0.1-1.1$, which will be discussed in Section 3.2.2.

As seen in Fig. 4(a), mode 2 disappears for $T/D > 1.3$ and mode 1 continues its appearance up to $T/D = 2.1$. The disappearance of mode 2 for $T/D > 1.3$ is also supported by the results of Gu and Sun (1999). The range $2.1 < T/D < 2.4$ is another bistable flow region at which the reattachment flow (mode 1) and a fully developed Karman vortex flow immediately behind the upstream cylinder switch from one to the other. However, they were sufficiently stable to be observed. This bistable flow resembles that which usually occurs in the case of two cylinders in tandem arrangement (Ishigai, 1972; Igarashi, 1981, 1984; Liu and Chen, 2002; Alam et al., 2002a, b, 2003c).

For $T/D > 2.4$, the Strouhal number for the upstream cylinder is the same as that of a single, isolated cylinder; however, two sets of Strouhal numbers are seen for the downstream cylinder. The Strouhal number values of the upper set are twice those of the lower set. The Strouhal number values of the lower set of the downstream cylinder are equal to those of the upstream cylinder, as occurs for two cylinders in tandem arrangement, i.e., the tandem effect. It is noted that the Strouhal number value of the upper set was detected only on the inner surface of the downstream cylinder, i.e., for the downstream cylinder, only one frequency (the lower one) was detected on the outer surface and the two frequencies were detected on the inner surface, as shown in Fig. 4(c). The appearance of the superharmonic frequency on the inner surface of the downstream cylinder for $T/D > 2.4$ attracted our attention and requires further elucidation. As we found in flow-visualization test results (not shown) and from the characteristics of the pressure signal, the superharmonic frequency on the inside surface of the downstream cylinder is due to an alternating impulse of two oncoming vortices from the upstream cylinder. As in a complete cycle of vortex shedding from the downstream cylinder, two opposite-sign vortices from the upstream cylinder are incident upon and/or pass over the inner surface of the downstream cylinder (as shown in Fig. 6), and the incident vortices cause a larger fluctuation of pressure on the inner surface of the downstream cylinder (Lee and Smith, 1991; Gursul and Rockwell, 1990), with a superharmonic frequency of twice the Strouhal frequency of the upstream cylinder. According to Sumner et al. (2000), the vortex impingement flow pattern appears on the downstream cylinder for arrangements near $\alpha \approx 25^\circ$ and for $T/D > 2.4$, i.e., the inner row of vortices shed from the upstream cylinder impinges upon the downstream cylinder and splits into two concentrations of vortices during the impingement process. However, splitting of vortices may occur only for limited configurations, as it is strongly dependent on the transverse offset of the downstream cylinder with respect to the incident vortex and degree of vorticity (Ziada and Rockwell, 1982; Gursul and Rockwell, 1990). As we found the superharmonic frequency on the inner surface only, it can be supposed that the inner row of vortices from the upstream cylinder fully dives to pass along the inner surface of the downstream cylinder, or the split vortices that pass by the inner surface are composed of a major share of mother vortices.

As shown in Fig. 7, a contour plot of the real part of the wavelet coefficient of a pressure signal at $\theta = -90^\circ$ of the downstream cylinder can manifest the existence of the superharmonic frequency described above. The positions of maximum and minimum intensity of energy in the wavelet map indicate the positions of peak and root, respectively, in the signal. It is clear that the pressure signal consists of two frequencies: the lower frequency ($St = 0.175$) is due to an alternating shedding of Karman vortices from the downstream cylinder, and the higher frequency ($St = 0.35$) having relatively lower energy is attributed to the incident vortices from the upstream cylinder. As we know, if a vortex is incident upon and/or passes over a point of a surface, the pressure at that point reaches a minimum value (maximum negative) when the vortex is closest to that point (Tang and Rockwell, 1983; Gursul and Rockwell, 1990). Hence, in the horizontal axis, the points of time at which the minimum energy (root) in the wavelet map are seen to occur at $St = 0.35$, are the times at which the incident vortices are closest to the point $\theta = -90^\circ$ of the downstream cylinder. It is

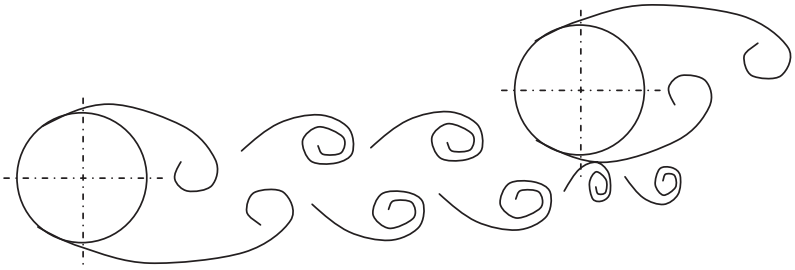

Fig. 6. Interaction of the incident vortices on the downstream cylinder, $T/D > 2.4$.

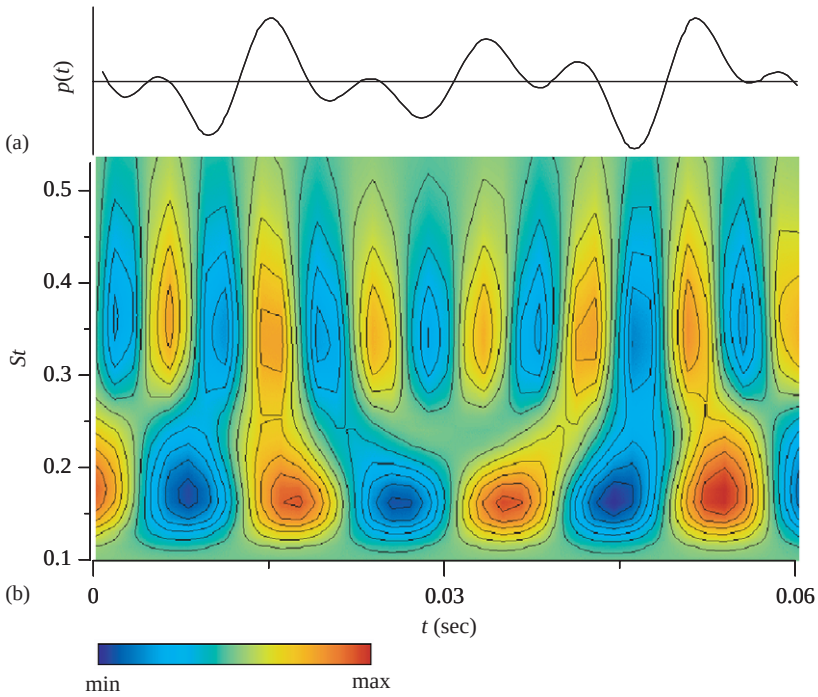

Fig. 7. Staggered configuration with $\alpha = 10^\circ$, $T/D = 3.5$: (a) instantaneous pressure signal of the downstream cylinder at $\theta = -90^\circ$; (b) real part of wavelet coefficients of signal (a), using Gabor wavelet.

interesting that, in one period at St = 0.175, i.e., in the range of time from one peak to the next peak at St = 0.175, two valleys (roots) occur at St = 0.35, implying two vortices incident upon the surface during a complete cycle of vortex shedding from the downstream cylinder.

3.2.2. *Staggered arrangement with $\alpha = 25^\circ$*

For $\alpha = 25^\circ$, the downstream cylinder always confronts a mean approaching flow, i.e., the downstream cylinder is outside of the inner shear layer of the upstream cylinder (Sumner et al., 2000). For such a case, the Strouhal numbers are shown in Fig. 8(a), together with the results of Kiya et al. (1980). Again note that the single, isolated cylinder Strouhal number value is 0.18 for the present case; the Reynolds numbers for the present case and for the case of Kiya et al. are 5.5×10^4 and 1.58×10^4, respectively. It is seen that both the cylinders have a synchronized lower frequency for $T/D < 1.1$, implying the two cylinders with regard to vortex-shedding frequency behave in a similar fashion to a single-bluff body (Kiya et al., 1980) though induced separation of gap flow from the downstream cylinder occurs (Sumner et al., 2000); only the outer shear layers of the two cylinders predominantly shed vortices in alternating fashion. The nature of the flow pattern for $T/D = 0.1-1.1$ can be assumed to be the same as that of mode 2 discussed in Section 3.2.1, at least with regard to vortex-shedding frequency.

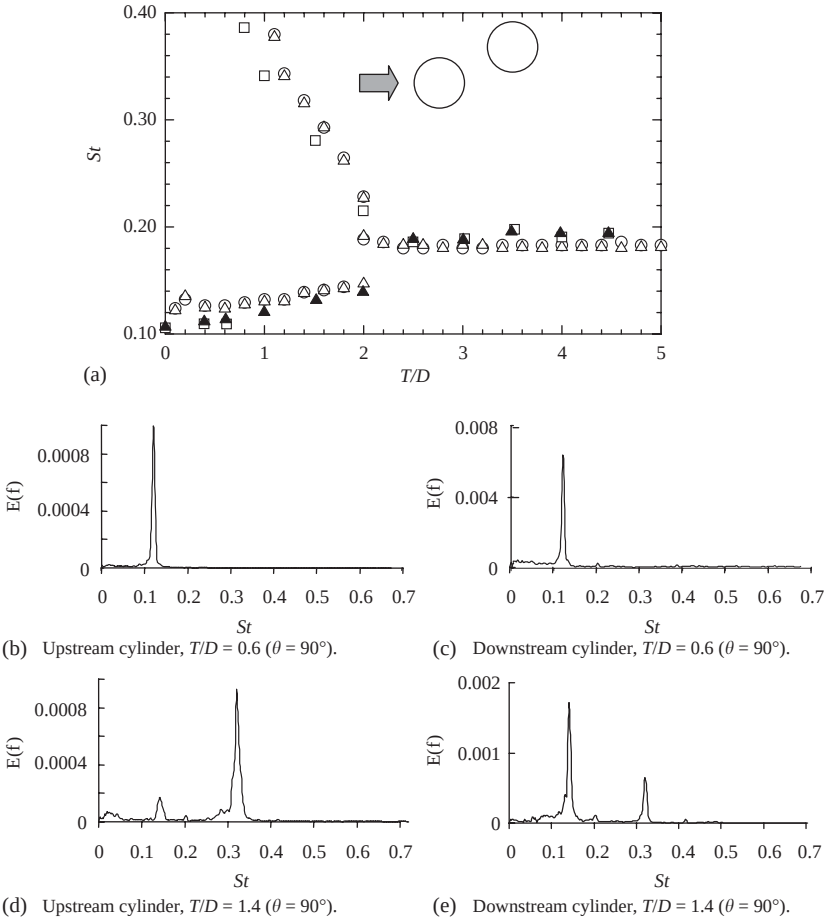

Fig. 8. (a) Strouhal number distributions for $\alpha = 25°$: ○, upstream cylinder; △, downstream cylinder; □, upstream cylinder (Kiya et al., 1980, $\alpha = 30°$); ▲, downstream cylinder (Kiya et al., 1980, $\alpha = 30°$); (b)–(e) power spectra of fluctuating pressures on the surfaces of the cylinders.

As observed in the flow pattern boundaries presented by Sumner et al. (2000) for two staggered cylinders, flow patterns involving 'induced separation (IS)' of gap flow and 'gap vortex pairing and enveloping (VPE)' phenomena can be expected in the range of $T/D = 0.1-1.1$, and a higher-frequency vortex shedding was found from the upstream cylinder for the IS and VPE flow patterns. However, in the present study, the higher frequency of vortex shedding was not detected in the power spectrum of fluctuating pressure on either side of the upstream cylinder for $T/D = 0.1-1.1$. Figs. 8(b,c), showing power spectra for $T/D = 0.6$, demonstrate that the frequencies of vortex shedding for both cylinders are the same, and there is no indication of a higher frequency for the upstream cylinder. It can be noted that the Reynolds number in the case of Sumner et al. (2000) was 850–1900, considerably smaller than that in the present case and that Kiya et al. (1980). Two peaks in the Fourier power spectra of the fluctuating pressure signals on either side of each cylinder were found for $T/D = 1.1-1.8$, so two values of Strouhal number for each of the cylinders are seen in the figure. In the range of $T/D = 1.1-1.8$, a share of the gap flow effectively rolls up immediately behind the upstream cylinder, resulting in formation of a narrower wake behind the upstream cylinder and a wider wake behind the downstream cylinder. Typical Fourier power spectra showing two Strouhal numbers for each of the cylinders are presented in Figs. 8(d) and (e). As seen in the Fourier power spectra, the level of energy at the higher Strouhal number of the upstream cylinder and at the lower Strouhal number of the downstream cylinder is greater. Only the higher Strouhal number for the upstream cylinder and only the lower Strouhal number for the downstream cylinder were found by other researchers (Ishigai et al., 1972; Kiya et al., 1980). Recently, Sumner and Richards (2003) have found such an appearance of two Strouhal numbers in the power spectra of fluctuating velocities in either of the two wakes, but why they have found two Strouhal numbers in the wake was left unexplained. It can be noted that, for the upstream cylinder, the energy level at the lower frequency in the Fourier power spectrum is relatively small and decreases with an

increase in T/D from 1.1 to 1.8. Similarly, for the downstream cylinder, the energy level at the higher frequency in the Fourier power spectrum is relatively small and decreases with an increase in T/D. The trends of Strouhal numbers obtained by Kiya et al. (1980) for $\alpha = 30^\circ$ show general agreement with those of the present results. The small difference in magnitudes of Strouhal number data between the two studies can be attributed to differences in experimental conditions, such as difference in stagger angle ($\alpha = 25^\circ$ and 30°), Reynolds number, turbulent intensity, blockage ratio and aspect ratio. However, Kiya et al. found only a higher frequency and a lower frequency for the upstream and downstream cylinders, respectively, for $T/D = 0.8-2$. The higher and lower frequencies for the upstream and downstream cylinders, respectively, agree with one's intuition, because narrower and wider wakes form behind the upstream and downstream cylinders, respectively (Ishigai, 1972; Kiya et al., 1980; Zdravkovich, 1977, 1987; Sumner et al., 2000).

Next we will discuss the nature of flow that causes two frequencies on either cylinder. Fig. 9 shows wavelet scalograms of fluctuating pressure signals for the upstream and downstream cylinders for $T/D = 1.40$. Note that the signals from the cylinders were stored simultaneously in order to acquire information on the mutual change of the flow patterns over the two cylinders. The pressure signals were at $\theta = 90^\circ$ for both the cylinders, i.e., they capture information on the characteristics of the outer shear layers only. The wavelet scalograms clearly show that the upstream and downstream cylinders shed vortices with a high intensity of energy when the frequency of vortex shedding is high and low, respectively. This is prevalent, but it is seen that the outer shear layer of the upstream cylinder frequently sheds

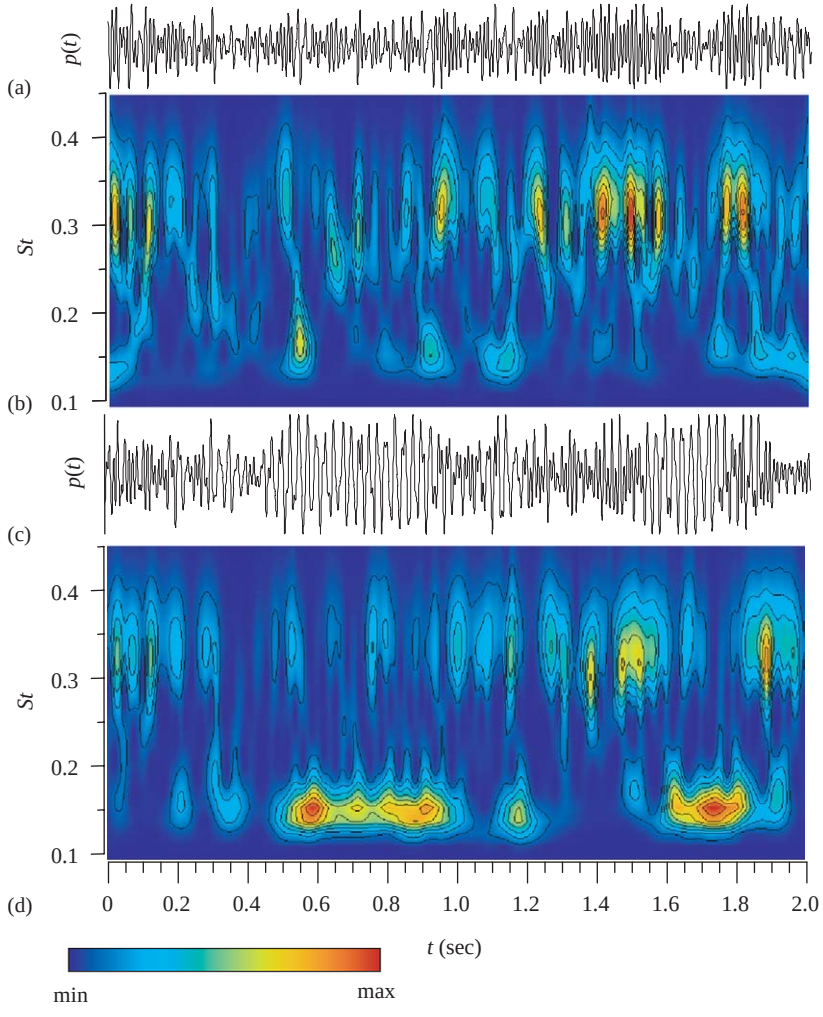

Fig. 9. Staggered configuration with $\alpha = 25^\circ$, $T/D = 1.4$: (a) pressure signal of the upstream cylinder at $\theta = 90^\circ$; (b) wavelet scalogram of signal (a); (c) pressure signal of the downstream cylinder at $\theta = 90^\circ$; (d) wavelet scalogram of signal (c). Signals (a) and (c) were stored simultaneously.The Morlet wavelet was used as the mother wavelet.

vortices at the lower frequency of the downstream cylinder and the outer shear layer of the downstream cylinder frequently sheds vortices at the higher frequency of the upstream cylinder. In other words, the vortex-shedding frequency of the upstream cylinder frequently locks-in at the lower frequency of the downstream cylinder, and the lower frequency of the downstream cylinder also frequently locks-in at the higher frequency of the upstream cylinder. However, the length of lock-in time for the upstream cylinder to shed vortices at the lower frequency of the downstream cylinder is comparatively shorter, and the length of lock-in time for the downstream cylinder to shed vortices with the higher frequency of the upstream cylinder is considerably longer. Mutual interactions of the four shear layers cause such a lock-in phenomenon. The lock-in of the frequency of the downstream cylinder with that of the upstream one can be attributed partly to the tandem effect (Section 3.1); as in the tandem arrangement, the downstream cylinder is forced to shed vortices at the frequency of the upstream cylinder. On the other hand, intermittent lock-in of the frequency of the upstream cylinder with that of the downstream cylinder can be explained as the intermittent appearance of the single bluff-body flow pattern with regard to vortex-shedding frequency (that appears for $T/D<1.1$, the lower Strouhal number for both cylinders) up to $T/D = 1.8$. It is very clear that there are three stable flow patterns for $T/D = 1.1-1.8$ with regard to the Strouhal numbers: (i) the flow with a higher Strouhal number for the upstream cylinder and a lower Strouhal number for the downstream cylinder ($t = 0.65-0.87$, 1.6–1.85 s, Fig. 9), (ii) the flow with a higher Strouhal number for both the cylinders: lock-in of downstream wake to the upstream one ($t = 0-0.2$, $1.25-1.6$ s, Fig. 9), and (iii) the flow with a lower Strouhal number for both the cylinders: lock-in of the upstream wake to the downstream one ($t = 0.5-0.65$, 0.87–0.95, 1.15–1.25 s, Fig. 9). It is also seen in the wavelet maps that, when the downstream cylinder locks-in to shed vortices at the higher frequency of the upstream cylinder, the energy level at the higher frequency of the upstream cylinder becomes greater, implying relatively stronger vortices are shed from the upstream cylinder when both the cylinders shed vortices with the higher frequency.

Now let us see what happens for the cases of the inner shear layers of the two cylinders. Wavelet scalograms and pressure signals at the inner surfaces ($\theta = -90^\circ$) of the two cylinders for $T/D = 1.40$ are shown in Fig. 10. These pressure signals are supposed to capture information on the characteristics of the inner shear layers. The nature of the wavelet scalogram of the upstream cylinder (Fig. 10(b)) is the same as that for $\theta = 90^\circ$ (Fig. 9(b)), implying that the characteristics of the inner and outer shear layers of the upstream cylinder with regard to vortex-shedding frequency and lock-in phenomenon are the same. Thus, the inner shear layer of the upstream cylinder sheds vortices in alternating fashion at the same frequencies of the outer shear layer of the same cylinder. An intriguing feature in Fig. 10 is that the frequency of the inner shear layer of the downstream cylinder is always locked-in/synchronized with that of the upstream cylinder: the inner shear layer of the downstream cylinder sheds vortices at the same frequency of the upstream cylinder. Such a synchronized vortex shedding from the inner shear layers of the cylinders was also observed in flow visualization tests by Sumner et al. (2000). Thus the wakes of the cylinders can be characterized mainly by the behavior of the outer shear layers. Now it can be inferred that, for $T/D = 1.1-1.8$: (i) the inner and outer shear layers of the upstream cylinder shed vortices at the same frequency and the inner shear layer of the downstream cylinder sheds vortices in synchronization with the inner shear layer of the upstream cylinder, (ii) the outer shear layer of the downstream cylinder generally sheds vortices at a lower frequency; however, it frequently locks-in to shed vortices at the higher frequency of the upstream cylinder, (iii) the two shear layers of the upstream cylinder and the inner shear layer of the downstream cylinder generally shed vortices with a higher frequency; however, they frequently lock-in to shed vortices at the lower frequency of the outer shear layer of the downstream cylinder.

From the above discussion, it is clear that the two shear layers of the downstream cylinder very often shed vortices at different frequencies. Now a satisfactory explanation of the lock-in of the frequencies of the shear layers can be presented. Consider as a reference the flow pattern in which the two shear layers of the upstream cylinder and the inner shear layer of the downstream cylinder shed vortices at the higher frequency. Since, in the reference flow pattern, the outer and inner shear layers of the downstream cylinder shed vortices at higher and lower frequencies, respectively, there may be a tendency for the two shear layers to shed vortices in alternating fashion at the same frequency. To shed vortices in alternating fashion, (i) the inner shear layer of the downstream cylinder may induce the outer shear layer (of the same cylinder) to be modified to shed vortices at the higher frequency of the inner shear layer, and (ii) the outer shear layer of the downstream cylinder may induce the inner shear layer (of the same cylinder) to be modified to shed vortices at the lower frequency. Now in the first case, when the outer shear layer of the downstream cylinder is modified to shed vortices at the higher frequency, all the shear layers of the two cylinders shed vortices at the same frequency (higher frequency), which has been termed as the lock-in of downstream wake to the upstream one. In the second case, the inner shear layer of the downstream cylinder is modified to shed vortices at the lower frequency of the outer shear layer of the same cylinder, and the inner shear layer of the downstream cylinder induces the inner shear layer of the upstream cylinder to shed vortices at the lower frequency because the inner shear layers of the two cylinders have a tendency to shed vortices in a synchronized state (Fig. 10). Finally, the inner shear layer of the upstream cylinder induces the outer shear layer of the upstream cylinder to shed vortices in alternating fashion at the lower frequency.

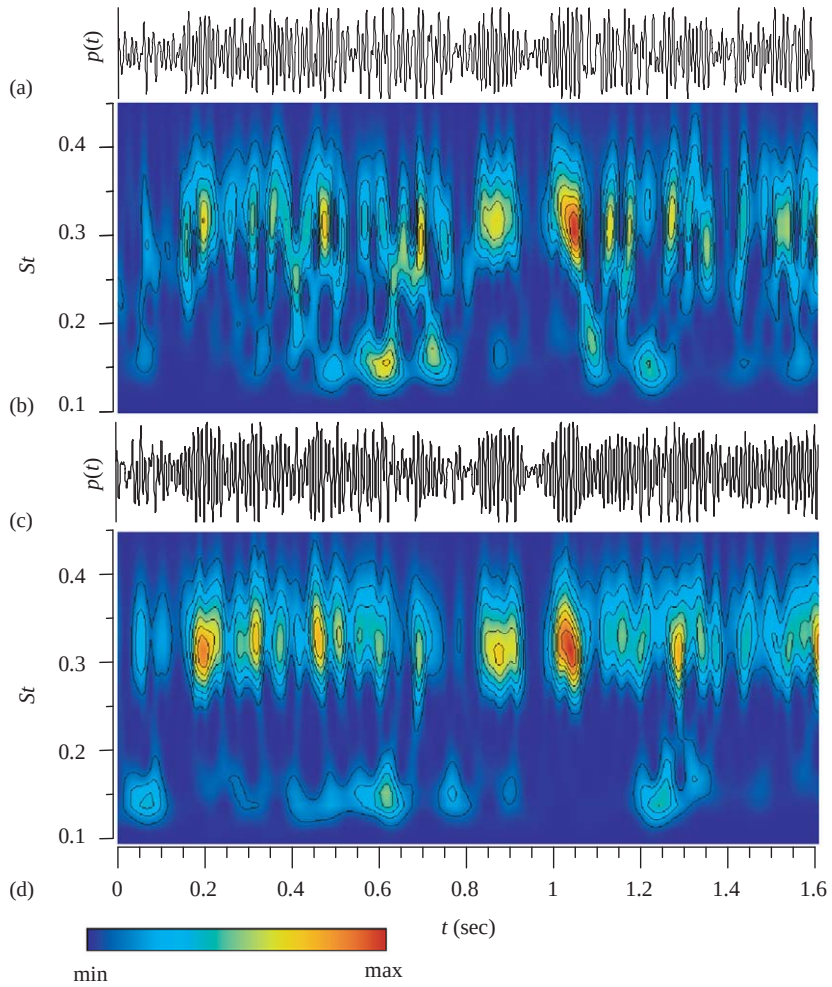

Fig. 10. Staggered configuration with $\alpha = 25^\circ$, $T/D = 1.4$: (a) instantaneous pressure signal of the upstream cylinder at $\theta = -90^\circ$; (b) wavelet scalogram of signal (a); (c) instantaneous pressure signal of the downstream cylinder at $\theta = -90^\circ$; (d) wavelet scalogram of signal (c). Results detained with the Morlet wavelet.

Thus now all the shear layers shed vortices at the lower frequency, which has been termed as the lock-in of the upstream wake to the downstream one.

Another striking feature seen in Fig. 8(a) is that the lower Strouhal number of the upstream cylinder disappears at $T/D = 2.0$; however, another Strouhal number equal to that of a single, isolated cylinder appears at $T/D = 2.0$ for both the cylinders. Therefore now, at $T/D = 2.0$, there exist two Strouhal numbers (0.228 and 0.188) for the upstream cylinder and three Strouhal numbers (0.228, 0.188 and 0.147) for the downstream cylinder. For $T/D > 2.0$, fully developed Karman vortices are generated from both the upstream and downstream cylinders, resulting in a Strouhal number equal to that of a single cylinder for both the cylinders. Such a jump or a drop of Strouhal number value from a lower or a higher one to a single-cylinder value is usually found to occur at the critical spacing of two cylinders in a tandem arrangement (Okajima, 1979; Igarashi, 1981, 1984; Alam et al., 2002a, b, 2003c) and has also been found for $\alpha = 10^\circ$ (Fig. 4(a)). The spacing $T/D = 2.0$ is the critical one, at which the flow with the narrower and wider wakes behind the upstream and downstream cylinders, respectively, changes to a fully developed Karman vortex flow behind both the cylinders. In other words, the flow patterns that appear for $1.1 \leqslant T/D < 2.0$ and for $T/D > 2.0$ appear in an irregular or intermittent fashion at $T/D = 2.0$. At $T/D = 2.0$, the lower and higher Strouhal numbers (0.147 and 0.228) of the downstream cylinder are contributed from the flow pattern for $T/D < 2.0$, and the intermediate Strouhal number (0.185) is contributed from the flow pattern for $T/D > 2.0$. The appearance of these Strouhal numbers at $T/D = 2.0$ can

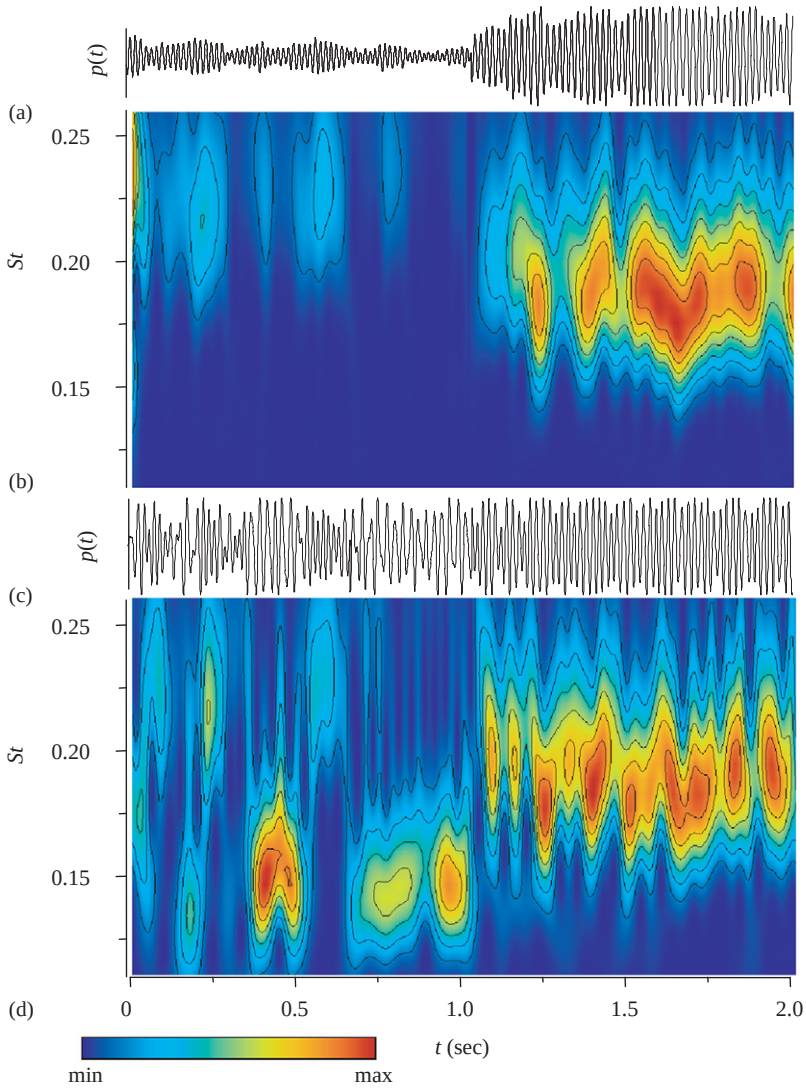

Fig. 11. Staggered configuration with $\alpha = 25^\circ$, $T/D = 2.0$: (a) instantaneous pressure signal of the upstream cylinder at $\theta = 90^\circ$; (b) wavelet scalogram of signal (a); (c) instantaneous pressure signal of the downstream cylinder at $\theta = 90^\circ$; (d) wavelet scalogram of signal (c). Results detained with the Morlet wavelet.

be explained from wavelet maps of the pressure signals stored simultaneously for $\theta = 90^\circ$, at the outer surfaces, as shown in Fig. 11. The wavelet maps clearly show that, for time $t < 1.05$ s, the upstream cylinder sheds vortices at a Strouhal number of 0.228 and the downstream cylinder sheds vortices at a Strouhal number of 0.147; however, the Strouhal number of the downstream cylinder frequently locks-in to the upstream cylinder Strouhal number. Thus, for $t < 1.05$ s, the existence of two frequencies for the downstream cylinder is corroborated. On the other hand, for $t > 1.05$ s, both the cylinders have a synchronized Strouhal number approximately equal to that of a single cylinder. Thus, the flow patterns for $t < 1.05$ and $t > 1.05$ s resemble those for $T/D < 2.0$ and $T/D > 2.0$, respectively. That is, at $t = 1.05$ s, the flow pattern appearing for $t < 1.05$ s discontinuously changes to that for $t > 1.05$ s. Hence, at $T/D = 2.0$, three different flow patterns with regard to Strouhal numbers are corroborated: (i) the flow with the higher and lower Strouhal numbers for the upstream and downstream cylinders, respectively, (ii) the flow with the higher Strouhal number for both the cylinders, and (iii) the flow with synchronized Strouhal numbers approximately equal to that of a single cylinder. Thus, a tristable nature flow appears at $T/D = 2.0$.

3.2.3. Staggered arrangement with $\alpha = 45^\circ$

The variation of Strouhal number with change in T/D for $\alpha = 45^\circ$ is shown in Fig. 12. There are many similarities and dissimilarities of the Strouhal number distribution for $\alpha = 45^\circ$ with that for $\alpha = 25^\circ$. Here also, for $T/D < 0.8$, the two cylinders behave like a single bluff-body with regard to vortex-shedding frequency. Sumner et al. (2000) observed a gap vortex pairing, splitting and enveloping flow pattern (VPSE) to persist for $T/D = 0.2-0.8$ and they detected a higher Strouhal number in the wake of the upstream cylinder for the VPSE flow pattern; however, only the lower Strouhal number on either side of the upstream cylinder was detected in the present study, as can be seen in Fig. 12(b). In this regard, the comment from the present authors is that only the outer shear layers of the two cylinders predominantly shed vortices in alternating fashion. Also, a constant phase lag of approximately 170° between the signals of fluctuating pressures on the outer surfaces ($\theta = 90^\circ$) of the two cylinders was found, confirming the alternating shedding of vortices from the outer shear layers. There are two values of the Strouhal number of the upstream cylinder in the range of $T/D = 0.8-2.1$, as seen in the figure. The evidence of the two Strouhal number values for the upstream cylinder is presented in Figs. 12(c, d). It is seen in the power spectra that the intensity of energy at the lower Strouhal number, compared with that of the higher Strouhal number, gradually decreases as T/D increases. Data presented by Sumner and Richards (2003) also show two peaks in the power spectra of fluctuating velocities in the wake of the upstream cylinder; however, they did not define the significance of the appearance of the two peaks. Such an appearance of two Strouhal numbers for the upstream cylinder was found for $\alpha = 25^\circ$ also (Section 3.2.2). Only one Strouhal number on either side surface of the downstream cylinder was found for $\alpha = 45^\circ$ (Fig. 12(e)) in contrast with two Strouhal numbers for $\alpha = 25^\circ$ (Fig. 8). That is, the intermittent lock-in of the downstream cylinder frequency to

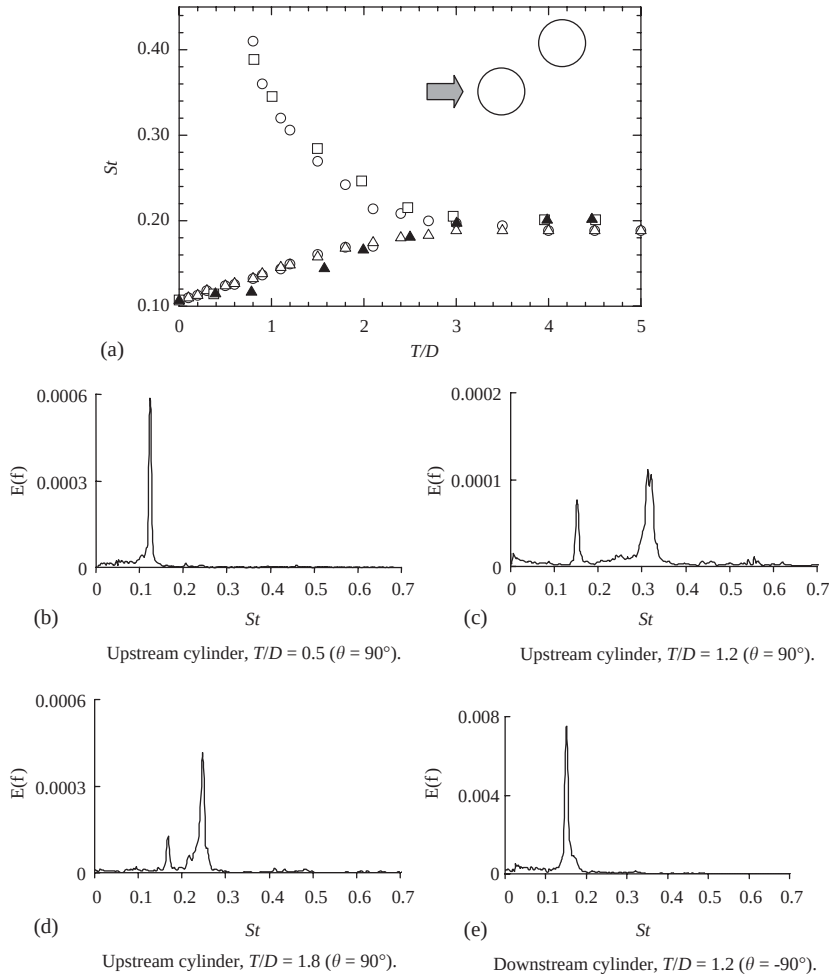

Fig. 12. (a) Strouhal number distributions for $\alpha = 45^\circ$: ○, upstream cylinder; △, downstream cylinder; □, upstream cylinder (Kiya et al., 1980); ▲, downstream cylinder (Kiya et al., 1980); (b)–(e) power spectra from fluctuating pressures.

that of the upstream one, the tandem effect, is completely absent for $\alpha = 45^\circ$. Power spectrum data published by Sumner and Richards (2003), however, show two peaks for the downstream cylinder for $\alpha = 45^\circ$ ($T/D = 1.0$) also, as found for $\alpha = 25^\circ$. An observation of their data suggests that the appearance of the higher Strouhal number for the downstream cylinder is highly dependent on the stagger angle α. The peak due to the higher Strouhal number of the downstream cylinder was absent for $\alpha > 45^\circ$ in their data. One may conjecture that this kind of lock-in phenomenon or the appearance of two Strouhal peaks was found in the present study, because of the low aspect ratio of the model. It has been mentioned that Sumner and Richards (2003) also found two peaks, though they estimated the Strouhal number from hot-wire signals in the cylinder wakes. In their case, the aspect ratio of the models was 24. Hence, the lock-in phenomenon and the multistable modes of vortex shedding are independent of aspect ratio and can be expected for more slender cylinders found in actual applications.

It is seen that the Strouhal number of the downstream cylinder and the higher Strouhal number of the upstream cylinder asymptotically approach the Strouhal number of a single, isolated cylinder with an increase in T/D. That is, as T/D increases, the narrower wake of the upstream cylinder and the wider wake of the downstream cylinder gradually change to become like that of a single, isolated, cylinder; whereas, for $\alpha = 25^\circ$, the higher and lower Strouhal numbers were suddenly merged at $T/D = 2.0$, beyond which the vortex-shedding process from either cylinder was almost similar to that of a single, isolated cylinder. For $T/D = 0.8-2.1$ (Fig. 12(a)), the appearance of two Strouhal numbers for the upstream cylinder and the change of Strouhal number of the upstream cylinder with respect to that of the downstream cylinder can be explained from wavelet scalograms of fluctuating pressures received simultaneously from the cylinders at $\theta = 90^\circ$ for the upstream cylinder and $\theta = -90^\circ$ for the downstream cylinder, as shown in Fig. 13. It is seen in the figure that the

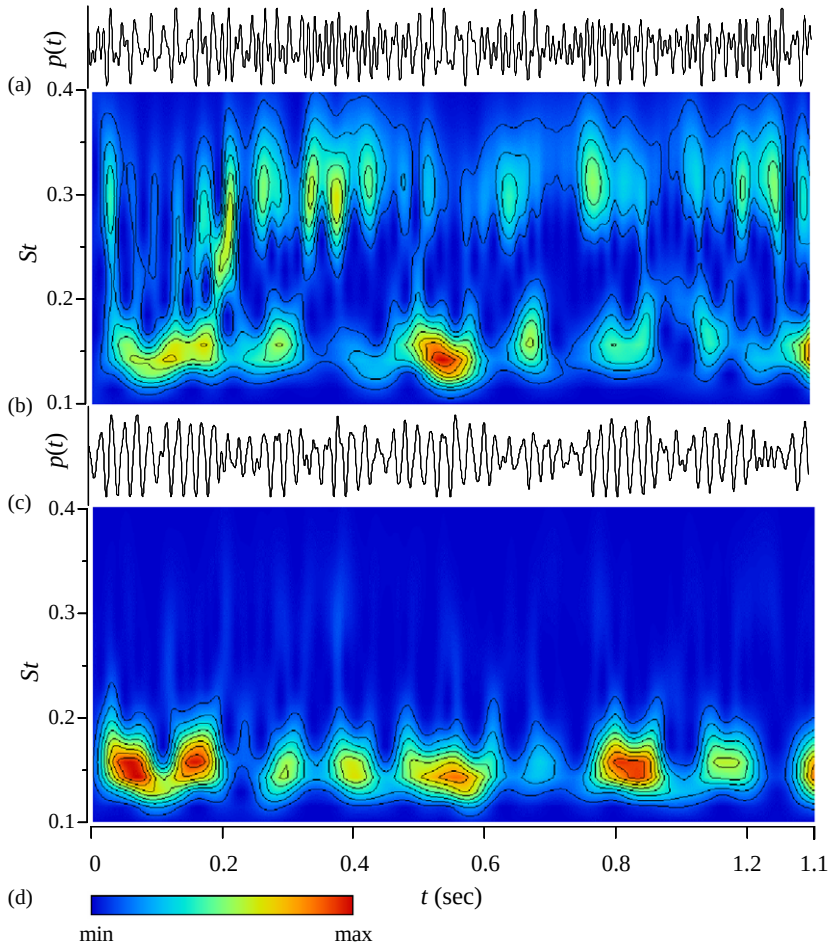

Fig. 13. Staggered configuration with $\alpha = 45^\circ$, $T/D = 1.2$: (a) instantaneous pressure signal of the upstream cylinder at $\theta = 90^\circ$; (b) wavelet scalogram of signal (a); (c) instantaneous pressure signal of the downstream cylinder at $\theta = -90^\circ$; (d) wavelet scalogram of signal (c). Results obtained with the Morlet wavelet.

downstream cylinder always sheds vortices at a lower Strouhal number of 0.15; the upstream cylinder sheds vortices at high and low Strouhal numbers of 0.305 and 0.15. That is, for $\alpha = 45^\circ$, the inner shear layer of the downstream cylinder does not shed vortices in synchronization with the inner shear layer of the upstream cylinder; rather, it sheds vortices in alternating fashion with the outer shear layer of the same cylinder. Note that the wavelet scalograms (not shown) of two pressure signals at $\theta = \pm 90^\circ$ of the upstream cylinder showed that the inner shear layer of the upstream cylinder always sheds vortices in an alternating fashion and at the same frequency of the outer shear layer of the same cylinder. It is conjectured that the upstream cylinder should shed vortices only at the higher Strouhal number, as found by other researchers. Indeed, the upstream cylinder very frequently locks-in to shed vortices with the lower Strouhal number of the downstream cylinder. Thus, two Strouhal numbers for the upstream cylinder prevail: the higher Strouhal number is due to the narrower wake and the lower one is due to synchronization with the downstream cylinder. The appearance of the lower Strouhal number of the upstream cylinder for $T/D = 0.8-2.1$ can also be explained as the continuation of the lower Strouhal number that appears for $T/D < 0.8$. That is, the flow pattern that appears for $T/D < 0.8$ continues its appearance intermittently for $T/D = 0.8-2.1$. It is also seen in the wavelet maps that, when the upstream cylinder locks-in with the downstream cylinder, i.e., when both cylinders shed vortices with the same frequency, the energy level in both the signals increases, indicating that a higher fluctuation of pressure occurs due to stronger shedding of vortices. It is interesting to note that, for $\alpha = 25^\circ$ ($T/D = 1.1-1.8$), the inner shear layer of the downstream cylinder always sheds vortices in synchronization with the inner shear layer of the upstream cylinder; however, for $\alpha = 45^\circ$ ($T/D = 0.8-2.1$), the inner shear layer of the downstream cylinder always sheds vortices in alternating fashion at the same frequency as the outer shear layer of the same cylinder. Sumner et al. (2000) grossly concluded that the two shear layers of the upstream cylinder and the inner shear layer of the downstream cylinder shed vortices at the same frequency for such a range of T/D. Indeed, the conclusion made by Sumner et al. is valid for $\alpha = 25^\circ$ (roughly 16–40°); in contrast, the inner shear layer of the downstream cylinder sheds vortices at the lower frequency in an alternating fashion with the outer shear layer of the same cylinder for $\alpha > 40^\circ$, as will be explained for $\alpha = 45^\circ$, 60° and 75°.

3.2.4. *Staggered arrangements with $\alpha = 60^\circ$ and 75°*

Strouhal number data for $\alpha = 60^\circ$ and 75°, together with data from Kiya et al. (1980), are plotted against T/D in Fig. 14. The results of the two studies are in agreement. However, for the present case, there are two Strouhal numbers for the upstream cylinder in the range of $T/D = 0.7$–1.5 and 0.5–1.2 for $\alpha = 60^\circ$ and 75°, respectively. The lower Strouhal number of the upstream cylinder is due to intermittent lock-in of the upstream cylinder to that of the downstream one, as has been discussed for $\alpha = 45^\circ$ (Section 3.2.3). Two peaks corresponding to the lower and higher Strouhal numbers of the upstream cylinder, in the power spectrum of fluctuating velocity in the outer side of the wake of the upstream cylinder for $\alpha = 60^\circ$ and 75° ($T/D = 1.0$), were also found by Sumner and Richards (2003). However, they did not ensure two Strouhal numbers for the upstream cylinder at $T/D = 1.5$. The measurement technique of the Strouhal number may be a cause of discrepancies between their data and those of the present study. Specifically, the present study was a near-field study using surface pressure measurements, while Sumner and Richards' study used a hot-wire anemometer at various positions in the cylinder wakes. The nature of the Strouhal number distributions for $\alpha = 60^\circ$ and 75° is the same as that for $\alpha = 45^\circ$ (Fig. 12). For $\alpha = 60^\circ$ and 75° also, the inner shear layer of the downstream cylinder does not synchronize with the inner shear layer of the upstream cylinder for $T/D > 0.7$ ($\alpha = 60^\circ$) or for $T/D > 0.5$ ($\alpha = 75^\circ$); indeed, it sheds vortices in alternating fashion with the outer shear layer of the same cylinder, as found for $\alpha = 45^\circ$.

Comparing the Strouhal number distributions for $\alpha = 45^\circ$, 60° and 75°, it is clear that, as α increases, the first appearance of the higher Strouhal number of the upstream cylinder occurs at a relatively lower spacing. However, when α reaches 90°, the appearance of the higher Strouhal number first occurs at $T/D = 0.4$ (Spivack, 1946), 0.5 (Bearman and Wadcock, 1973; Kiya et al., 1980), and 0.2 (Alam et al., 2003a). Also, data for $\alpha = 45^\circ$, 60° and 75° reveal that the higher and lower Strouhal numbers asymptotically approach the single-cylinder value with increasing T/D; however, gradients of the higher and lower sets of Strouhal numbers with respect to T/D, to reach to the single cylinder value, increase with increasing α. It can also be noted that, as α increases from 45° to 75°, the lock-in range of T/D of the upstream cylinder Strouhal number with that of the downstream cylinder becomes shorter, and such a lock-in phenomenon is completely absent for the side-by-side arrangement. Further investigations at some intermediate values of α between 75° and 90° are necessary to reveal how much the lock-in range becomes shorter and when it is first absent.

3.3. *A square cylinder and a circular cylinder in staggered arrangement*

In the case of two circular cylinders, many new interesting phenomena have been found in this study for $\alpha = 25^\circ$; the Strouhal number distributions for $\alpha = 45^\circ$, 60° and 75° were almost the same in nature. The new interesting phenomena attracted our attention to investigate what happens if a square cylinder and a circular cylinder are placed in staggered

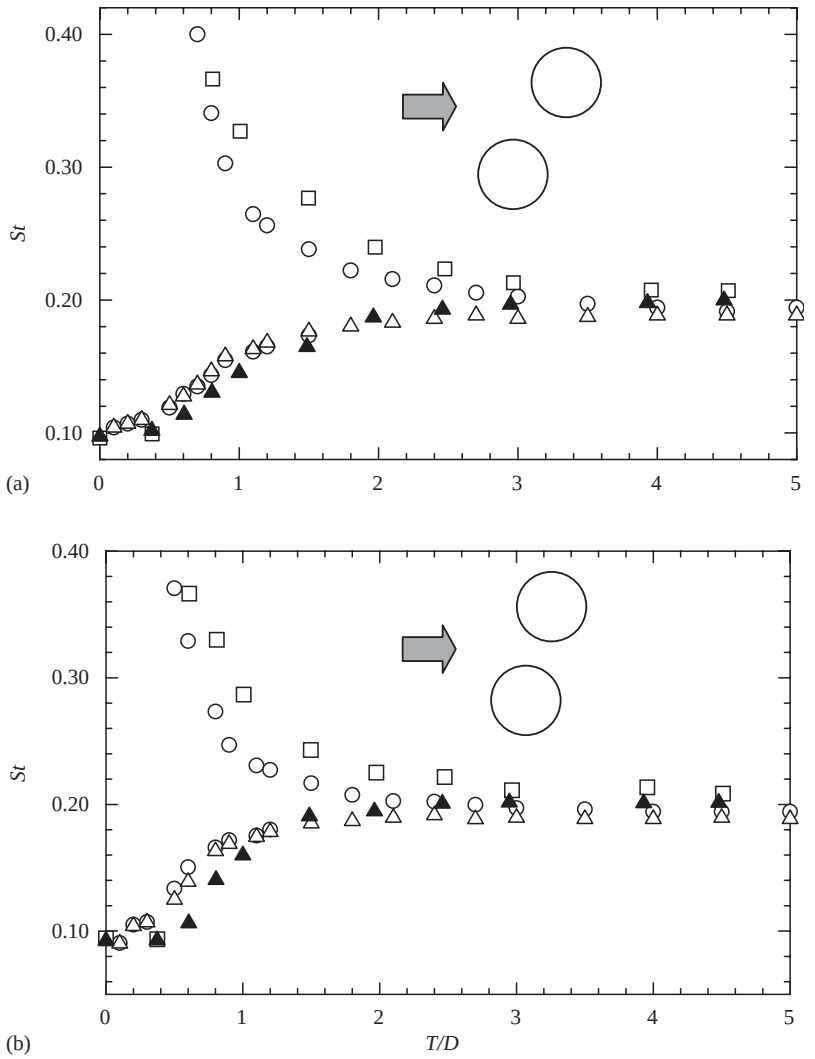

Fig. 14. Strouhal number distributions: (a) $\alpha = 60^\circ$, (b) $\alpha = 75^\circ$: ○, upstream cylinder; △, downstream cylinder; □, upstream cylinder (Kiya et al., 1980); ▲, downstream cylinder (Kiya et al., 1980).

arrangement. It is intuitive that a square cylinder forms a wider and stronger wake than a circular cylinder and that their Strouhal numbers, when isolated, are different from each other. So, the interference between the two near-wakes, with regard to vortex-shedding frequency, of a square cylinder and a circular cylinder in staggered arrangement is expected to be different from that of two circular cylinders. To satisfy our curiosity, a square cylinder and a circular cylinder in staggered arrangements with $\alpha = 25^\circ$ and 60° were investigated to corroborate the new findings and to be differentiated from those involving two circular cylinders. For $\alpha = 25^\circ$, when a circular cylinder and a square cylinder are used as the upstream and downstream ones, respectively, and when their positions are reversed, Strouhal number data obtained from fluctuating surface pressures are shown in Fig. 15. Fig. 15(a) is for the case when the circular cylinder is used as the upstream one, and 15(b) is for the case when the square cylinder is used as the upstream one. Note that the Strouhal numbers were estimated based on the upstream cylinder dimension. It is seen that the trend of the Strouhal numbers, when the circular cylinder is upstream (Fig. 15(a)), is similar to that for two circular cylinders (Fig. 8(a)); however, in this case, the lower Strouhal number of the upstream cylinder in the range $T/D = 1.3-2.2$ is absent; whereas for the case of the two circular cylinders with $\alpha = 25^\circ$, both a higher and lower Strouhal numbers prevailed for the upstream cylinder. Thus, when a square cylinder is used as the downstream cylinder, frequency lock-in of the upstream cylinder to that of the downstream cylinder does not occur. For the downstream (square) cylinder,

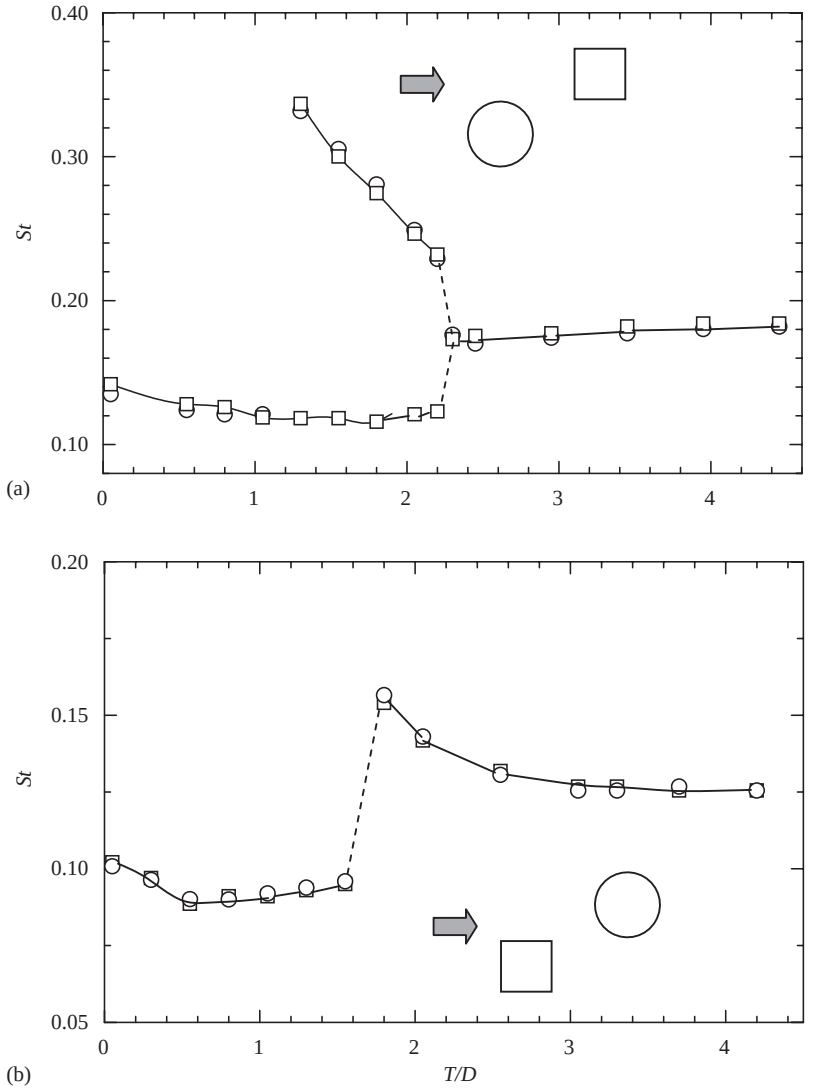

Fig. 15. Strouhal number distributions for $\alpha = 25^{\circ}$: (a) circular cylinder is at the upstream of square cylinder, (b) square cylinder is at the upstream of circular cylinder : ○, circular cylinder; □, square cylinder. Strouhal number was calculated based on the upstream cylinder.

however, two sets of Strouhal numbers in the range of $T/D = 1.3-2.2$ are seen. The lower set of Strouhal numbers of the downstream cylinder is due to a wider wake formed behind the downstream cylinder, and the higher set of the Strouhal numbers is due to an intermittent lock-in of the downstream cylinder frequency to that of the upstream cylinder, as has been discussed for the case of two circular cylinders with $\alpha = 25^{\circ}$. It is important to mention that here the inner shear layer of the downstream cylinder was found to shed vortices in synchronization with the frequency of the upstream cylinder, and two frequencies were found only for the outer shear layer of the downstream cylinder, implying the outer shear layer of the downstream cylinder generally sheds vortices with the lower Strouhal number and it frequently locks-in to shed vortices in synchronization with the higher Strouhal number of the upstream cylinder as well as with the inner shear layer of the same cylinder. For $T/D > 2.3$, at which a fully developed Karman vortex forms behind the upstream cylinder with a Strouhal number of 0.18 (single circular cylinder value), the downstream cylinder, whose single cylinder Strouhal number value is 0.125, is forced to shed vortices in synchronization with the incident vortices from the upstream cylinder.

When the square cylinder is used as the upstream one (Fig. 15(b)), the Strouhal number distributions are quite different from those in Figs. 15(a) and 8(a). Here the two cylinders behave like a single bluff-body, with regard to

vortex-shedding frequency, for a longer range of T/D (<1.8), because the square cylinder forms a relatively wider wake than a circular cylinder. When the gap flow effectively forms a narrower wake behind the upstream cylinder at $T/D = 1.8$, the Strouhal number of the upstream cylinder jumps to a higher value. Then the Strouhal number of the upstream cylinder gradually decreases and reaches its single-cylinder Strouhal number value at $T/D = 3$. When the upstream cylinder has a narrower wake for $T/D = 1.8-3.0$, the downstream cylinder should shed vortices at a lower Strouhal number as found for the case of two circular cylinders (Fig. 8(a)) and for the case of a circular cylinder upstream with a square cylinder downstream (Fig. 15(a)); but the lower Strouhal number of the downstream cylinder is absent here. This means that the wake of the downstream circular cylinder is in a continuously locked-in state with the relatively stronger wake of the upstream cylinder when a square is used as the upstream cylinder, where as intermittent lock-in was found for the case of the two circular cylinders and for the case when a circular cylinder is upstream of a square cylinder. Thus the lock-in of wake frequency, when two wakes are nearer, is a unique phenomenon; however, it depends on the strength of the upstream wake.

Similarly, Strouhal number distributions for a square cylinder and a circular cylinder arranged in staggered with $\alpha = 60^\circ$ are shown in Fig. 16. In Fig. 16(a), when the circular cylinder is used as the upstream cylinder, the trend of

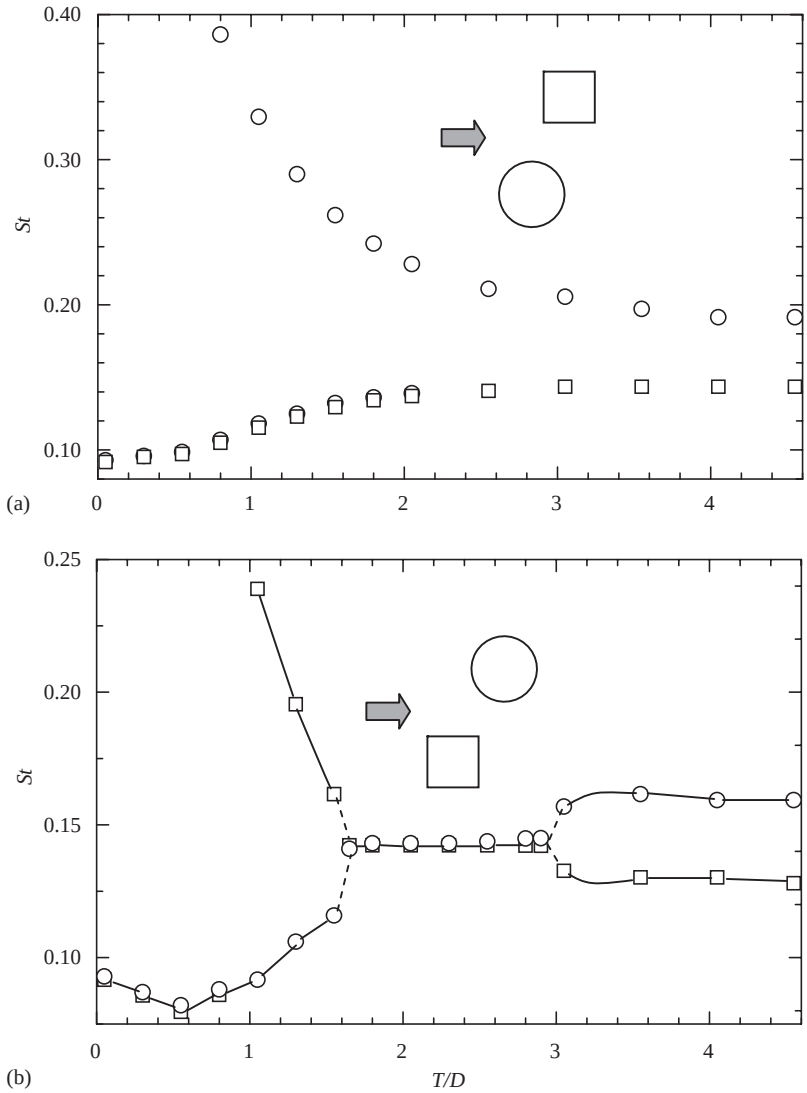

Fig. 16. Strouhal number distributions for $\alpha = 60^\circ$: (a) circular cylinder is at the upstream of square cylinder, (b) square cylinder is at the upstream of circular cylinder : ○, circular cylinder; □, square cylinder. Strouhal number is calculated based on the upstream cylinder diameter or width.

Strouhal number variation is almost the same as that of two circular cylinders case (Fig. 14(a)). Here, for $T/D = 0.8-2.1$, intermittent lock-in of the upstream cylinder frequency with that of the downstream cylinder occurs; thus two Strouhal number values for the upstream cylinder are presented in the figure. For the two-circular-cylinder case, the higher and lower Strouhal numbers asymptotically merge to a single cylinder value; however, in this case (Fig. 16(a)), the higher and lower Strouhal numbers do not merge, because their single-cylinder Strouhal-number values are different. Indeed, the Strouhal numbers of both the cylinders approach their single cylinder value. It is seen that there is no interference effect between the cylinders for $T/D > 3.5$.

However, when the square cylinder is used as the upstream cylinder (Fig. 16(b)), the Strouhal number distributions are quite different from those of two circular cylinders (Fig. 14) or from those when a circular cylinder is upstream of a square cylinder with $\alpha = 60^\circ$ (Fig. 16(a)). In this case (Fig. 16(b)), the gap flow effectively produces a narrower wake behind the upstream cylinder, corresponding to a higher Strouhal number of 0.24 at $T/D = 1.0$. Then the Strouhal number of the upstream cylinder gradually decreases to approach that of a single square cylinder, and the Strouhal number of the downstream cylinder gradually increases to reach that of a single circular cylinder. However, when the difference between the Strouhal numbers of the two cylinders becomes small, the Strouhal number value of the upstream cylinder and that of the downstream cylinder suddenly drops and jumps, respectively, to an intermediate Strouhal number value at $T/D = 1.6$, to be synchronized with each other. The Strouhal numbers of the upstream and downstream cylinders are synchronized for $T/D = 1.6-2.9$, then they suddenly separate and attain their single cylinder values. Thus, the lock-in of the two near wakes of two staggered cylinders, a tendency to generate vortices at the same frequency, is a common characteristic of the flow. Further research on two square cylinders and combinations of a square cylinder and a circular cylinder in staggered arrangement could be carried out to reveal further interesting phenomena of the shear layer interactions of two bluff bodies.

4. Conclusions

The Strouhal frequencies of two identical circular cylinders in staggered configurations at $\alpha = 10^\circ$, 25°, 45°, 60°, and 75° in the range of $T/D = 0.1-5.0$ were investigated at a Reynolds number of 5.5×10^4. Also, measurements of the Strouhal frequencies of a square cylinder and a circular cylinder in tandem and in certain staggered arrangements have been presented in this paper. The Strouhal frequencies were measured for individual shear layers from fluctuating surface pressures on the cylinders. The main results of the present study are summarized as follows.

(i) For $\alpha = 10^\circ$, the downstream cylinder always sheds vortices at the same frequency as the upstream cylinder, that usually occurs in the tandem configuration. However, a bistable flow appears for the range of $T/D = 0.1-1.3$, in which two flow patterns, mode 1 (Pattern II_B) and mode 2, (Pattern III_B) switch from one to the other. Such a kind of bistable flow is consistent with that previously found by Gu and Sun (1999). Mode 1 corresponds to a higher Strouhal number of about 0.47 for both the cylinders, and mode 2 corresponds to a lower Strouhal number of 0.09 for both the cylinders. For $T/D > 2.4$, each of the cylinders sheds vortices in similar fashion to a single cylinder and at the same frequency of a single cylinder; however, a superharmonic frequency of twice the Strouhal frequency of the upstream cylinder is detected on the inside surface of the downstream cylinder. An interaction of the incident vortices from the upstream cylinder onto the inner surface of the downstream cylinder causes such a superharmonic frequency on the inside surface of the downstream cylinder. The superharmonic frequecny is elucidated from the results of a wavelet analysis of the pressure signal.

(ii) For $\alpha = 25^\circ$, in the range $0.1 \leqslant T/D < 1.1$, the two cylinders behave like a single bluff body, at least with regard to vortex-shedding frequency; only the outer shear layers of the two cylinders predominantly shed vortices at a lower Strouhal number. In the range of $T/D = 1.1-1.8$, where a share of the gap flow effectively rolls up immediately behind the upstream cylinder resulting in the generation of a narrower wake behind the upstream cylinder and a wider wake behind the downstream cylinder, both of the shear layers of the upstream cylinder generally shed vortices in an alternating fashion at a higher Strouhal number, but they frequently lock-in to shed vortices with the lower Strouhal number of the outer shear layer of the downstream cylinder. Similarly, the outer shear layer of the downstream cylinder generally sheds vortices at a lower Strouhal number, but it frequently locks-in to shed vortices at the higher Strouhal number of the upstream cylinder. Also, the inner shear layer of the downstream cylinder always sheds vortices in synchronization with the inner shear layer of the upstream cylinder. Therefore, three stable flow patterns with regard to vortex-shedding frequency persist for $T/D = 1.1-1.8$. These are: (a) the flow with a higher Strouhal number for the upstream cylinder and a lower Strouhal number for the downstream cylinder, (b) the flow with a higher Strouhal number for both the cylinders: lock-in of downstream wake to the upstream one, and (c) the flow with a lower Strouhal

number for both the cylinders: lock-in of upstream wake to the downstream one. At $T/D = 2.0$, the lower and higher Strouhal numbers suddenly merge to an intermediate Strouhal number equal to that of a single, isolated cylinder.

(iii) For $\alpha = 45^\circ$, in the range of $T/D = 0.8-2.1$, the inner shear layer of the downstream cylinder does not shed vortices in synchronization with the inner shear layer of the upstream cylinder; rather, it sheds vortices in an alternating fashion with the outer shear layer of the same cylinder. Here, only the shear layers of the upstream cylinder frequently lock-in to shed vortices at the lower frequency of the downstream cylinder. Hence, two stable flow patterns with regard to Strouhal numbers persist for $T/D = 0.8-2.1$. These are: (a) the flow with a higher Strouhal number for the upstream cylinder and a lower Strouhal number for the downstream cylinder, and (b) the flow with a lower Strouhal number for both the cylinders: lock-in of upstream wake to the downstream one.

(iv) Strouhal number distributions for $\alpha = 60^\circ$ and 75° are almost the same in nature as those of $\alpha = 45^\circ$. Here also, at the intermediate range of T/D, only the shear layers of the upstream cylinder frequently lock-in to shed vortices at the lower frequency of the downstream cylinder, and the inner shear layer of the downstream cylinder always sheds vortices in an alternating fashion with the outer shear layer of the same cylinder.

(v) The multistable flow patterns and the lock-in phenomenon are elucidated from the results of a wavelet analysis of fluctuating pressures simultaneously measured on the surfaces of the two cylinders. Wavelet analysis is a very useful tool for analyzing multistable flow, the lock-in phenomenon and the mutual change of two flows with respect to time.

(vi) When a square cylinder and a circular cylinder are arranged at $\alpha = 25^\circ$, with the square cylinder being used as the upstream cylinder, the downstream cylinder always sheds vortices in synchronization with the upstream cylinder. For $\alpha = 60^\circ$, when the square cylinder is used as the upstream cylinder, the two cylinders are found to be locked-in to shed vortices at an intermediate Strouhal number for a certain range of values of T/D.

Acknowledgments

The first author wants to express his gratitude to Associate Professor Masaru Moriya for his continuous help in discussing experimental results and to Mr K. Takai for his assistance in computer work. The authors also wish to thank technical officer Mr Y. Obata for his expertise in the precise fabrication of the models.

References

Alam, M.M., Moriya, M., Takai, K., Sakamoto, H., 2002a. Suppression of fluid forces acting on two circular cylinders in a tandem arrangement by passive control of flow. In: Hwung, H.H., Lee, J. F., Hwang, K.S. (Eds.), Proceedings of the Fifth International Conference on Hydrodynamics, Taiwan, pp. 235–240.

Alam, M.M., Moriya, M., Takai, K., Sakamoto, H., 2002b. Suppression of fluid forces acting on two square cylinders in a tandem arrangement by passive control of flow. Journal Fluids and Structures 16, 1073–1092.

Alam, M.M., Moriya, M., Sakamoto, H., 2003a. Aerodynamic characteristics of two side-by-side circular cylinders and application of wavelet analysis on the switching phenomenon. Journal Fluids and Structures 18, 325–346.

Alam, M.M., Sakamoto, H., Moriya, M., 2003b. Reduction of fluid forces acting on a single circular cylinder and two circular cylinders by using tripping rods. Journal Fluids and Structures 18, 347–366.

Alam, M.M., Moriya, M., Takai, K., Sakamoto, H., 2003c. Fluctuating fluid forces acting on two circular cylinders in a tandem arrangement at a subcritical Reynolds number. Journal of Wind Engineering and Industrial Aerodynamics 91, 139–154.

Bearman, P.W., Wadcock, A.J., 1973. The interaction between a pair of circular cylinder normal to a stream. Journal of Fluid Mechanics 61, 499–511.

Bokaian, A., Geoola, F., 1984. Wake-induced galloping of two interfering circular cylinders. Journal of Fluid Mechanics 146, 383–415.

Chen, S.S., 1986. A review of flow-induced vibration of two circular cylinders in crossflow. ASME Journal of Pressure Vessel Technology 108, 382–393.

Cimbala, J.M., Krein, M.V., 1990. Effect of freestream conditions on the far wake of a circular cylinder. AIAA Journal 28, 1369–1373.

Daubechies, I., 1990. The wavelet transform, time-frequency localization and signal analysis. IEEE Transactions, Information Theory 36, 961–1005.

Farge, M., 1992. Wavelet transforms and their applications to turbulence. Annual Review of Fluid Mechanics 24, 395–457.

Gu, Z., Sun, T., 1999. On interference between two circular cylinders in staggered arrangement at high subcritical Reynolds numbers. Journal of Wind Engineering and Industrial Aerodynamics 80, 287–309.

Gu, Z.F., Sun, T.F., He, D.X., Zhang, L.L., 1993. Two circular cylinders in high-turbulence flow at supercritical Reynolds number. Journal of Wind Engineering and Industrial Aerodynamics 49, 379–388.

Guillaume, D.W., LaRue, J.C., 1999. Investigation of the flopping regime with two-, three- and four-cylinder arrays. Experiments in Fluids 27, 145–156.

Gursul, I., Rockwell, D., 1990. Vortex street impinging upon an elliptical leading edge. Journal of Fluid Mechanics 211, 211–242.

Hamdan, M.N., Jubran, B.A., Shabaneh, N.H., Abu-Samak, M., 1996. Comparison of various basic wavelets for the analysis of flow-induced vibration of a cylinder in cross-flow. Journal of Fluids and Structures 10, 633–651.

Hori, E., 1959. Experiments on flow around a pair of parallel circular cylinders. Proceeding of Ninth Japan National Congress for Applied Mechanics, paper III-11, pp. 231–234.

Igarashi, T., 1981. Characteristics of the flow around two circular cylinders arranged in tandem (1st Report). Bulletin of the Japan Society of Mechanical Engineers 24, 323–331.

Igarashi, T., 1984. Characteristics of the flow around two circular cylinders arranged in tandem (2nd Report). Bulletin of the Japan Society of Mechanical Engineers 27, 2380–2387.

Ishigai, S., Nishikawa, E., Nishimura, E., Cho, K., 1972. Experimental study of structure of gas flow in tube banks axes normal to flow. Bulletin of the Japan Society of Mechanical Engineers 15, 949–956.

Kamemoto, K., 1976. Formation and interaction of two parallel vortex streets. Bulletin of the Japan Society of Mechanical Engineers 19, 283–290.

Kareem, A., Kijewski, T., 2002. Time-frequency analysis of wind effects on structures. Journal of Wind Engineering and Industrial Aerodynamics 190, 1435–1452.

Kiya, M., Arie, M., Tamura, H., Mori, H., 1980. Vortex shedding from two circular cylinders in staggered arrangement. ASME Journal of Fluids Engineering 102, 166–173.

Ko, N.W.M., Wong, P.T.Y., 1992. Flow past two circular cylinders of different diameters. Journal of Wind Engineering and Industrial Aerodynamics 41–44, 563–564.

Konstantinidis, E., Balabani, S., Yianneskis, M., 2002. A study of vortex shedding in a staggered tube array for steady and pulsating cross-flow. ASME Journal of Fluids Engineering 124, 737–746.

Lee, D.J., Smith, C.A., 1991. Effect of vortex core distortion on blade-vortex interaction. AIAA Journal 29, 1355–1363.

Lesage, F., Gartshore, I.S., 1987. A method of reducing drag and fluctuating side force on bluff bodies. Journal of Wind Engineering and Industrial Aerodynamics 25, 229–245.

Li, H., 1997. Wavelet auto-correlation analysis applied to eddy structure identification of free turbulent shear flow. The Japan Society of Mechanical Engineers International Journal 40, 567–576.

Li, H., 1998. Flow structure identification of a turbulent shear flow with use of wavelet statistics. CD-ROM Proceedings of the Eighth International Symposium on Flow Visualization, Italy, No.145, pp. 145.1–145.11.

Li, H., Nozaki, T., 1997. Application of wavelet cross-correlation analysis to a plane turbulent jet. The Japan Society of Mechanical Engineers International Journal 40, 58–66.

Liu, C.H., Chen, J.M., 2002. Observations of hysteresis in flow around two square cylinders in a tandem arrangement. Journal of Wind Engineering and Industrial Aerodynamics 90, 1019–1050.

Mahir, N., Rockwell, D., 1996. Vortex formation from a forced system of two cylinders, Part II: side-by-side arrangement. Journal of Fluids and Structures 10, 491–500.

Nakagawa, S., Nitta, K., Senda, M., 1999. An experimental study on unsteady turbulent near wake of a rectangular cylinder in channel flow. Experiments in Fluids 27, 284–294.

Newland, D.E., 1993. An Introduction of Random Vibrations, Spectral and Wavelet Analysis, third ed. Longman Scientific and Technical, London.

Okajima, A., 1979. Flow around two tandem circular cylinders at very high Reynolds numbers. Bulletin of the Japan Society of Mechanical Engineers 22, 504–511.

Price, J., 1976. The origin and nature of the lift force on the leeward of two bluff bodies. Aeronautical Quarterly 26, 154–168.

Price, S.J., Paidoussis, M.P., 1984. The aerodynamic forces acting on groups of two and three circular cylinders when subject to a cross-flow. Journal of Wind Engineering and Industrial Aerodynamics 17, 329–347.

Schewe, G., 1983. On the force fluctuations acting on a circular cylinder in cross-flow from subcritical up to transcritical Reynolds numbers. Journal of Fluid Mechanics 133, 265–285.

Spivack, H.M., 1946. Vortex frequency and flow pattern in the wake of two parallel cylinders at varied spacing normal to an air stream. Journal of Aeronautical Science 13, 289–301.

Sumner, D., Richards, M.D., 2003. Some vortex-shedding characteristics of the staggered configuration of circular cylinders. Journal of Fluids and Structures 17, 345–350.

Sumner, D., Price, S.J., Paidoussis, M.P., 2000. Flow-pattern identification for two staggered circular cylinders in cross-flow. Journal of Fluid Mechanics 411, 263–303.

Sun, T.F., Gu, Z.F., He, D.X., Zhang, L.L., 1992. Fluctuating pressure on two circular cylinders at high Reynolds number. Journal of Wind Engineering and Industrial Aerodynamics 41–44, 77–588.

Tang, Y.P., Rockwell, D., 1983. Instantaneous pressure fields at a corner associated with vortex impingement. Journal of Fluid Mechanics 126, 187–204.

Torrence, C., Compo, G., 1998. A practical guide to wavelet analysis. Bulletin of American Meteorological Society 79, 61–78.

Yilmaz, T., Kodal, A., 2000. An analysis on coaxial jet flows using different decomposition techniques. Journal of Fluids and Structures 14, 359–373.

Yong, R.K., 1998. Wavelet Theory and its Application, sixth ed. Kluwer Academic Publishers, Dordrecht, The Netherlands.

Zdravkovich, M.M., 1977. Review of flow interference between two circular cylinders in various arrangement. ASME Journal of Fluids Engineering 199, 618–633.

Zdravkovich, M.M., 1980. Aerodynamics of two parallel circular cylinders of finite height at simulated high Reynolds numbers. Journal of Wind Engineering and Industrial Aerodynamics 6, 59–71.

Zdravkovich, M.M., 1981. Review and classification of various aerodynamic and hydrodynamic means for suppressing vortex shedding. Journal of Wind Engineering and Industrial Aerodynamics 7, 145–189.

Zdravkovich, M.M., 1987. The Effects of interference between circular cylinders in cross flow. Journal of Fluids and Structures 1, 239–261.

Zdravkovich, M.M., Pridden, D.L., 1977. Interference between two circular cylinders; series of unexpected discontinuities. Journal of Industrial Aerodynamics 2, 255–270.

Ziada, S., Rockwell, D., 1982. Vortex-leading-edge interaction. Journal of Fluid Mechanics 118, 79–107.